

Disordered complex networks : energy optimal lattices and persistent homology

S. Ghosh ^{*} N. Miyoshi [†] T. Shirai [‡]

Abstract

Disordered complex networks are of fundamental interest in statistical physics, and they have attracted recent interest as stochastic models for information transmission over wireless networks. While mathematically tractable, a network based on the regulation Poisson point process model offers challenges vis-a-vis network efficiency. Strongly correlated alternatives, such as networks based on random matrix spectra (the Ginibre network), on the other hand offer formidable challenges in terms of tractability and robustness issues. In this work, we demonstrate that network models based on random perturbations of Euclidean lattices *interpolate* between Poisson and rigidly structured networks, and allow us to achieve the *best of both worlds* : significantly improve upon the Poisson model in terms of network efficacy measured by the *Signal to Interference plus Noise Ratio* (abbrv. SINR) and the related concept of *coverage probabilities*, at the same time retaining a considerable measure of mathematical and computational simplicity and robustness to erasure and noise.

We investigate the optimal choice of the base lattice in this model, connecting it to the celebrated problem optimality of Euclidean lattices with respect to the Epstein Zeta function, which is in turn related to notions of lattice energy. This leads us to the choice of the triangular lattice in 2D and face centered cubic lattice in 3D, whose Gaussian perturbations we consider. We provide theoretical analysis and empirical investigations to demonstrate that the coverage probability decreases with increasing strength of perturbation, eventually

^{*}Dept. of Mathematics, National University of Singapore, subhrowork@gmail.com

[†]Dept. of Math. & Comp. Sc., Tokyo Instt. of Tech., miyoshi@is.titech.ac.jp

[‡]Institute of Math. for Industry, Kyushu University, shirai@imi.kyushu-u.ac.jp

converging to that of the Poisson network. In the regime of low disorder, our studies suggest an approximate statistical behaviour of the coverage function near a base station as a log-normal distribution with parameters depending on the Epstein Zeta function of the lattice, and related approximate dependencies for a power-law constant that governs the network coverage probability at large thresholds.

In 2D, we determine the disorder strength at which the perturbed triangular lattice (abbrev. PTL) and the Ginibre networks are the *closest* measured by comparing their network topologies via a comparison of their *Persistence Diagrams* in the total variation as well as the symmetrized nearest neighbour distances. We demonstrate that, at this very same disorder, the PTL and the Ginibre networks exhibit very similar coverage probability distributions, with the PTL performing at least as well as the Ginibre. Thus, the PTL network at this disorder strength can be taken to be an effective substitute for the Ginibre network model, while at the same time offering the advantages of greater tractability both from theoretical and empirical perspectives.

Contents

1	Introduction and main ideas	3
1.1	Stochastic spatial networks	3
1.1.1	Spatial networks and wireless communications	3
1.1.2	Disordered complex networks	4
1.1.3	Poissonian networks and spatial independence	5
1.1.4	Spatial dependence and Ginibre networks	6
1.1.5	Hyperuniformity and spatial networks	7
1.2	A three-fold investigative framework	7
1.3	Disordered lattices	8
1.4	The network observables	10
1.4.1	The basic set-up	10
1.4.2	The SINR and its distribution	10
1.4.3	Rayleigh fading and related effects	11
1.4.4	SINR for disordered lattices	12
1.5	Main results and contributions	14
2	SINR in extremal parameter regimes	17
2.1	The regime of small σ : generalities	17

2.2	The regime of small σ : a log-normal approximation	19
2.3	The regime of small σ and large θ : parametric dependencies of coverage probability	22
2.4	The regime of small σ and small θ : asymptotic linearity . . .	23
2.5	Monotonicity in σ	24
3	Choice of lattice and energy optimality	25
4	Comparison of random point sets and persistent homology	26
4.1	Comparison via persistent diagrams	26
4.2	Comparison via nearest neighbour distribution	29
5	Disordered lattices for optimal SINR in 2D and 3D	30
5.1	2D planar networks	30
5.2	3D spatial networks	32
6	Interpolation with Poisson in the high noise regime	36
7	Concluding remarks	37
8	Proofs of Theorems 1.4 and 6.1	38
8.1	Proof of Theorem 1.4	38
8.1.1	Justification of the interchange of integration and limit	40
8.2	Proof of Theorem 6.1	42
9	Acknowledgements	44
A	Appendix : Persistent homology and persistence diagrams	45
B	Appendix : Comparison of nnd-s of 2D & 3D point sets	49

1 Introduction and main ideas

1.1 Stochastic spatial networks

1.1.1 Spatial networks and wireless communications

The study of complex networks to understand and enhance wireless communication has attracted considerable interest in recent years. An important

driving force behind this trend has been the exponentially growing volumes of data that are being generated and gathered, and the necessity of physical infrastructure to make the communication and collection of such data practicable.

An important feature of wireless communication networks is their spatial nature ([19, 5, 2]). Namely, the network consists of a large number of nodes that are distributed in space - typically 2 or 3 dimensional Euclidean space, although more exotic geometries have also been investigated ([38, 64]). This endows such networks with an inherent structure - e.g., in 2D they can be studied as (weighted) planar graphs, and therefore inherit all the characteristics possessed by such special classes of mathematical structures. Each of the nodes, or base stations, broadcast signals that interfere with each other; and an important objective is to understand how the field of signal strength at various locations, adjusted with the interferences, looks like across the ambient space. A particular goal would be to design network layouts that optimize such signal strength for most (or typical) locations.

1.1.2 Disordered complex networks

In the study of large complex systems, a classical ansatz, particularly in the physical sciences, is to consider an analogous random system. The typical behaviour of the random system is believed to provide a good insight for how the large complex system will behave, particularly in terms of its relatively simple, readily measurable characteristics. A celebrated example of this approach is the famous random matrix model proposed by Wigner ([62]) to understand the behaviour of large and complex nuclei. It turns out that the distribution of energy levels of the nuclei of large and complex atoms are captured extremely well by the spectral properties of random matrices, a phenomenon referred to as the *Wigner surmise* ([63, 43]).

In the setting of large, complex networks, this approach can be executed via spatial random point process models. The use of random point processes to study the spatial distribution of wireless network models has been a popular topic in the recent years ([4, 9, 46]). In these models, random points sampled from an appropriate underlying distribution are thought of as representing the locations of wireless nodes. Various objects of interest, like the signal to noise ratio, are studied as random variables, and their asymptotic behaviour in the limit of the system size tending to infinity analysed in order to understand its efficacy as a communication network.

1.1.3 Poissonian networks and spatial independence

The most popular and widely studied model in this respect is the Poisson point process ([4, 9, 32]). A key feature of the Poisson point process is that the statistical distributions of the points in disjoint domains are statistically independent ([37]). This makes the Poisson point process the analogue of *pure noise* in the world of point processes. Another consequence of this property is that it makes it rather convenient to do computations with the Poisson point process - indeed, closed form expressions can be derived for almost any statistic of interest, and very often asymptotics can be studied in considerable detail.

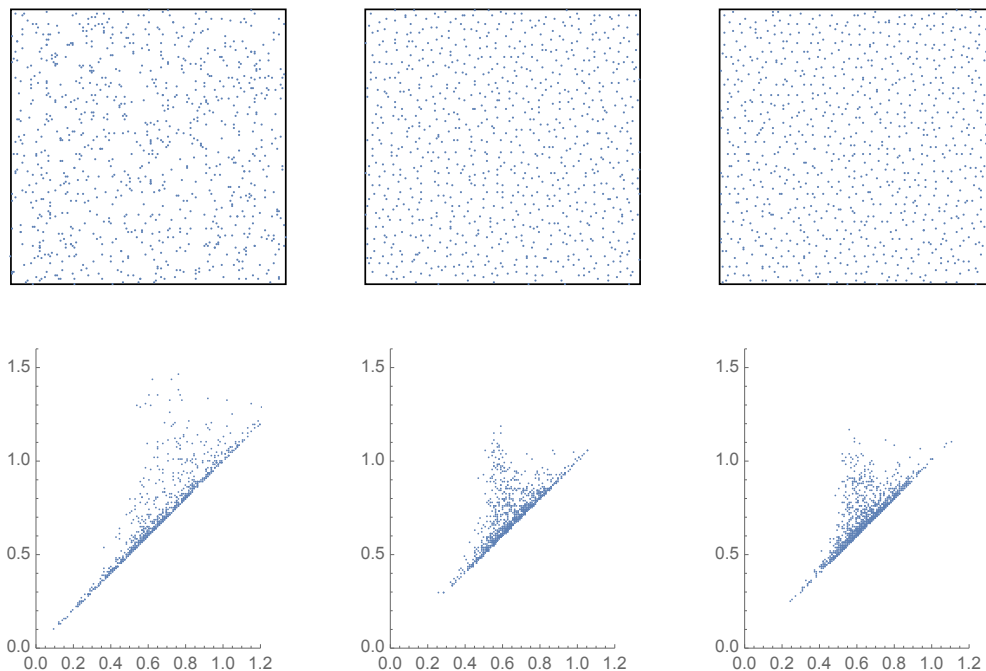


Figure 1: Upper panel: from left to right, simulations of Poisson, Ginibre and Perturbed Triangular Lattice (PTL) ($\sigma = 0.4$) with unit intensity. Lower panel: the persistence diagrams of the above.

However, the very same property of statistical independence becomes a limitation if we think of the real-life modelling perspective. Indeed, the spatial independence implies that, given that there is a node at a location,

the next node to be introduced is equally likely to occur very close to or far away from it. This leads to the formation of clusters of points in the Poisson point process, and to compensate for such clusters since the average number of points is held fixed at some constant, we have large vacant spaces devoid of any Poisson points (see Fig. 1 top left). Intuitively, this reduces the efficacy of the Poisson point process as a model for wireless network, making the coverage somewhat non-uniform and leading to an unnecessary excess of coverage in certain patches and lack thereof in certain others. This can, in fact, be established rigorously by comparing certain relevant statistics of the Poisson point process with those of competing models ([34]).

1.1.4 Spatial dependence and Ginibre networks

This motivates the study of models of random point sets which are bereft of these difficulties. The point process to be used as a model must satisfy two basic criteria, which are often somewhat contradictory in spirit. First of all, the point process must allow sufficiently strong spatial correlation so as to induce mutually repulsive behaviour at local scales and thereby preclude the clumping behaviour as the Poisson point process which renders the latter rather ineffectual as a model for wireless networks. On the other hand, it must have sufficiently nice properties as a mathematical model so that key statistical quantities can be estimated and theoretical or numerical analyses can be carried out effectively. A related criterion, which is important from an application-oriented perspective, is that the point process should be easy to simulate, so that large scale statistical behaviour can be gleaned from simulations, in case theoretical computations do not yield sufficiently tractable expressions (which is often the case in non-Poisson situations).

An important model of point processes which has been studied in this respect is the so-called Ginibre ensemble ([44, 17, 41]), which can also be looked upon as the 2D Coulomb gas (or the 2D One Component Plasma) at the inverse temperature $\beta = 2$ ([27, 35]). Introduced by the physicist Ginibre as the non-Hermitian analogue of the famous Wigner Gaussian random matrix ensemble ([29]), it belongs to the special class of point processes known as *determinantal point processes* (or DPPs) ([52, 34]). In the rest of this article, we will occasionally refer to it as the Ginibre ensemble and the resulting network as the *Ginibre network*. Via the connection to either random matrices or DPPs, it may be seen that mutual repulsion between the points is a built-in feature of the Ginibre network ([34]). Moreover, for quan-

tities which involve only the absolute values of the points like the coverage probability or link success probability, we can exploit the fact the process of absolute values has an equivalent description as independent gamma random variables ([34]), which enables some facility with theoretical analysis.

1.1.5 Hyperuniformity and spatial networks

Qualitatively, one can think of *regularity* in a point process as relatively *uniform* distribution of points over space as opposed to a uniform distribution in a probabilistic sense, arising out of the strength of spatial correlations - e.g., the tension between local repulsion pushing points away from each other, and a constraint on their average density being held fixed. In the recent literature, such behaviour have been studied in its own merit, under the broad umbrella of *hyperuniformity*, and related *rigidity phenomena*.

Hyperuniformity, also referred to as *superhomogeneity*, is the phenomenon of suppressed fluctuations of particle numbers - in Poissonian systems, the variance of the number of points in a large domain of space grows like the volume (referred to in the physics literature as *extensive fluctuations*), whereas for hyperuniform systems, the fluctuations are smaller order of the volume (resp., *sub-extensive*), often growing only like the surface area of the domain ([59, 27]). This is exhibited by many important systems in nature, a key example being that of random matrix ensembles including the Ginibre ensemble discussed above, Coulomb systems in general, as well as more exotic models like zeros of random functions ([34, 27]) and *stealthy hyperuniform systems* ([60, 58, 28]). An alternate description of hyperuniformity can be obtained via its “structure function” or “power spectrum” $S(k)$. Roughly speaking, it is the Fourier transform of the (truncated) two point correlation function of the point process. Hyperuniformity entails that $S(k) \rightarrow 0$ as $k \rightarrow 0$, and indeed an array of hyperuniform behaviour can be obtained depending on the rate at which $S(k) \rightarrow 0$ as $k \rightarrow 0$ ([59, 27, 3]).

1.2 A three-fold investigative framework

The above considerations open up the avenue for investigation from three perspectives. First of all, while the Ginibre network is more spatially regular than the Poisson network, it is not the only such model, and therefore it is a natural question to investigate whether other models can provide additional value from the network design perspective, while retaining the benefit of a

relatively regular point pattern. In particular, considering hyperuniformity as a cornerstone of a spatially regular point pattern, we can investigate models of random point sets which exhibit similar hyperuniform behaviour as the Ginibre point process, but offer other advantages from the modelling and analysis points of view.

Secondly, in the Ginibre network, the lack of independence of any sort other than the distances of the points from the origin turns out to be a hindrance for theoretical analysis as well as computational investigations.

Finally, the Ginibre ensemble is more or less a stand-alone model, and it is difficult to introduce a rich class of parameters so as to leave open the possibility of tuning the model to data. From a statistical modelling point of view, a parametric family would thus be of great interest. Another specificity of the Ginibre ensemble is its planarity, with no natural extensions to higher dimensions, wherein such network models would be significant particularly in 3D space.

In summary, it would be of great interest to investigate point process models of wireless networks that embody the spatial regularity features of the random matrix ensemble, while at the same time retain the benefits of the Poissonian networks with regard to an independent latent structure for computation, simulation and analytical purposes, and to be able to do so in a parametric manner in general dimensions.

1.3 Disordered lattices

In this article, we study a class of models which are promising candidates for attaining many of objectives outlined above. To this end, we consider a lattice $\Lambda \subset \mathbb{R}^d$ for any arbitrary dimension d , and a mean-zero random variable γ with distribution F on \mathbb{R}^d . We can then define the point process

$$\mathcal{P}_{\Lambda, \gamma} = \{n + \gamma_n : n \in \Lambda, \gamma_n \text{ i.i.d. copies of } \gamma \sim F\}.$$

Here a subset $\Lambda \subset \mathbb{R}^d$ is said to be a lattice in \mathbb{R}^d if Λ is an additive group of \mathbb{R}^d which is expressed as

$$\Lambda = \left\{ \sum_{i=1}^d a_i \mathbf{e}_i : a_i \in \mathbb{Z} \ (i = 1, 2, \dots, d) \right\}$$

by using a basis $\mathbf{e}_1, \dots, \mathbf{e}_d$ of the vector space \mathbb{R}^d . A particularly interesting case of this arises when γ is Gaussian on \mathbb{R}^d with mean 0 and variance σ^2 ,

entailing that σ automatically becomes a tuning parameter in the model. Another important consideration is the choice of the lattice Λ , which, as we shall see in Section 3, will have a significant impact on the Signal to Interference plus Noise Ratio and will lead to interesting mathematical connections with energy optimality. Finally, as demonstrated in Section 6, disordered Gaussian lattices interpolate continuously between the original lattice and the Poisson point process with the same density, as the noise parameter σ varies. This provides us the opportunity to tune the parameter σ so as to achieve a desired balance between structure and randomness in the network.

The lattice group Λ acts on \mathbb{R}^d by translations and its quotient $T_\Lambda := \mathbb{R}^d/\Lambda$ turns out to be a torus, which is represented by its fundamental parallelootope of Λ

$$\mathcal{D}_\Lambda = \left\{ \sum_{i=1}^d a_i \mathbf{e}_i : a_i \in [0, 1) \ (\forall i = 1, 2, \dots, d) \right\}.$$

If one desires to have translation invariance of the perturbed lattice, one can add a uniform shift by adding a uniform random vector from \mathcal{D}_Λ . It turns out that such $\mathcal{P}_{\Lambda, \gamma}$ is hyperuniform as soon as the “tail” of γ (i.e., $\mathbb{P}[|\gamma| > t]$) decays faster than t^{-d} , where $|\gamma|$ is the Euclidean norm in \mathbb{R}^d . For a theoretical discussion of this property, we refer the reader to [27, 26]. Since the effect of the uniform shift on SINR appears just as the integration over \mathcal{D}_Λ , for simplicity of our discussions, we will omit it in the present paper.

The above models, in spite of exhibiting *rigid structure* or *regularity*, as manifested in their hyperuniform behaviour, have an independence structure clearly built into them. The fact that the particles tracing their origin to different lattice points in Λ are independent enables us to write down closed form expressions for various statistics of interest, and also facilitates an ease of simulation that is not available with the Ginibre random network.

Although we have introduced the models with i.i.d. perturbations, an interesting variant is one where the perturbations are independent but not identically distributed, by varying the scale parameter (i.e. the standard deviation of γ), or for that matter, considering different random variables for perturbing different lattice locations. This can be utilized to factor in spatial inhomogeneity of a wireless network node distribution.

One can, for example, consider a statistical problem of fitting a lattice perturbation model as above to a given wireless network, by estimating parameters like the standard deviations of Gaussian fluctuations in different

lattice sites, or if one is more ambitious, estimating the statistical properties of an unknown distribution of perturbation that might belong to a wider family like the exponential family. It is very difficult to formulate a reasonable analogue of such questions in the context of other strongly correlated models.

Finally, an important advantage of perturbed lattice processes in modelling wireless base stations is that these processes are robust to missing data and erasure. To be more precise, if a collection of perturbed lattice points are missing or corrupted, they can be re-generated by simply re-sampling the perturbations corresponding to those particular lattice points, with the rest of the configuration being left unchanged, and this procedure fully preserves the statistical properties of the random network. This is an important practical advantage that sets disordered lattice processes apart from other correlated point processes like random matrix processes, where erasure or corruption of a subset of points do not admit any simple correction.

1.4 The network observables

1.4.1 The basic set-up

We are now ready to define the key observables of the induced network that we are going to study, which we will do in the completely general set up of an arbitrary point process.

Our setting is the following. A configuration $\Phi = \sum_{i=1}^{\infty} \delta_{X_i}$ is a simple (stationary) point process on \mathbb{R}^d and it provides a realization of spatial configuration of base stations of a cellular network. A decreasing function $\ell : (0, \infty) \rightarrow [0, \infty)$ is a *path-loss function*, which represents the attenuation of signals at distance r . A random variable F_i , independent of the point process Φ , represents a random effect of fading/shadowing from the base station X_i to the typical user. Here we assume the so-called *Rayleigh fading*, i.e., $\{F_i\}_{i=1}^{\infty}$ are i.i.d. exponential random variables with mean 1. Let W be a random variable representing *thermal noise* (modelling general random disturbances from the *environment*), independent of $\{F_i\}_{i=1}^{\infty}$ and Φ .

1.4.2 The SINR and its distribution

Suppose that a typical user is located at the origin (since our point processes are translation invariant, statistically there is no loss of generality in reducing

to the origin as the point of reception), and is receiving the signal associated with the nearest base station X_B from the origin, where B is the lattice site corresponding to the nearest base station. This signal is being retarded by interference from other base stations, and by the pure thermal noise W . The Signal-to-Interference-plus-Noise-Ratio (henceforth abbreviated as SINR) at the origin is defined by

$$\text{SINR}_o = \frac{F_B \ell(|X_B|)}{W + I(B)} \left(= \frac{\text{signal}}{\text{noise}} \right), \quad (1.1)$$

where $I(B) = \sum_{i \neq B} F_i \ell(|X_i|)$ is the cumulative interference signal from all the base stations other than B . SINR_o is the observable by which we are going to adjudicate the efficiency of the network, and hence this quantity will of paramount interest in our considerations. For detailed considerations on this model, including its motivational origins and effectiveness, we refer the interested reader to ([4, 44]).

Notice that, because of the randomness in the locations of the base stations, SINR_o is a random variable. In order to compare SINR_o for two random networks, we compare their tails, that is, the probability that the SINR_o exceeds a certain level θ . This probability is known as the *coverage probability* (corresponding to the level θ), and greater the coverage probability for a given θ , better is the network.

In the set-up of signal, interference and noise discussed above, the coverage probability is given by

Proposition 1.1 (Proposition 2.2 in [45]). Suppose that base stations are distributed according to a simple point process $\Phi = \sum_{i=1}^{\infty} \delta_{X_i}$. Then, the coverage probability is given by the formula

$$P(\text{SINR}_o > \theta) = E \left[\prod_{j \neq B} \left(1 + \theta \frac{\ell(|X_j|)}{\ell(|X_B|)} \right)^{-1} \right], \quad (1.2)$$

where X_B is of the least modulus among the base station locations.

1.4.3 Rayleigh fading and related effects

In particular, in the important case when $\ell(r) = ar^{-2\beta}$ ($\beta > 1$) and the spatial dimension 2, the coverage probability $p_c(\theta, \beta)$ is given by

$$p_c(\theta, \beta) := P(\text{SINR}_o > \theta) = E \left[\prod_{j \neq B} \left(1 + \theta \left| \frac{X_B}{X_j} \right|^{2\beta} \right)^{-1} \right]. \quad (1.3)$$

In general dimension $d \geq 2$, a natural choice for the path-loss is $\ell(r) = ar^{-d\beta}$ ($\beta > 1$), and it turns out that

$$p_c(\theta, \beta) = E \left[\prod_{j \neq B} \left(1 + \theta \frac{|X_B|^{d\beta}}{|X_j|^{d\beta}} \right)^{-1} \right]. \quad (1.4)$$

In this work, as also with natural applications, we mostly concern ourselves with dimensions 2 and 3.

Remark 1.2. More generally, we can consider the SINR at a general point a , possibly different from the origin. This will be given by

$$\text{SINR}_a = \frac{F_B \ell(|X_B - a|)}{W + I(B; a)} \left(= \frac{\text{signal at } a}{\text{noise at } a} \right), \quad (1.5)$$

where X_B is the nearest base station to a , and $I(B; a) = \sum_{i \neq B} F_i \ell(|X_i - a|)$ is the cumulative interference signal from all the base stations other than B , observed at a . Expressions analogous to (1.2) and (1.3) can also be obtained. In particular, we have the following expression for the coverage probability at the location a :

$$p_c^{[a]}(\theta, \beta) = E \left[\prod_{j \neq B} \left(1 + \theta \frac{|X_B - a|^{d\beta}}{|X_j - a|^{d\beta}} \right)^{-1} \right], \quad (1.6)$$

where B is the nearest base station to a . In particular, this focusses attention on the *coverage function* at the location a . For a point configuration Φ obtained by a random perturbation of the lattice Λ , the coverage function at a is the random variable

$$\mathcal{C}(\Phi; a) = \prod_{B \neq j \in \Lambda} \left(1 + \theta \frac{|X_B - a|^{d\beta}}{|X_j - a|^{d\beta}} \right)^{-1}. \quad (1.7)$$

1.4.4 SINR for disordered lattices

It can already be understood from Eq. (1.3) why negatively dependent (i.e., mutually repelling) point configurations would be effective in improving the coverage probability. To this end, we focus on the terms $\left(1 + \theta \left| \frac{X_B}{X_j} \right|^{2\beta} \right)^{-1}$. In order that the value of such a term be high, two things would be conducive.

First, $|X_B|$ should be preferably low. Secondly, the most important terms that can damp the coverage probability are those for which $|X_j|$ is small subject to the constraint that $|X_j| > |X_B|$, and the contribution of these terms should be not too small, which essentially requires that there are not too many X_j that are farther than X_B from the origin but not too far. This necessitates that points do not cluster close to the sphere in \mathbb{R}^d on which the nearest base station is located.

For repulsive point processes, typically the nearest point to the origin is closer to the origin with a higher probability. This is corroborated by the fact that the *hole probability* for radius R (i.e., the probability of having no points inside a ball of radius R) typically decays faster than the Poisson point process ([34]). For the nearest base station to be far away from the origin, there has to be a big *hole* centred at the origin, which is statistically unfavourable in repulsive point processes. Furthermore, negatively dependent processes also statistically discourage clustering of points in a region of space. These two properties of repulsive point processes help in improving the coverage probability, and make them ideal candidates for base station distribution in wireless networks.

As discussed in Section 1.3, our main focus in this work is on random networks where the base stations are distributed as a disordered lattice. Let Λ be a lattice in \mathbb{R}^d . We consider the following probability density function on $t \geq 0$, indexed by $n \in \Lambda$:

$$f(t, n, \sigma) = e^{-\frac{|n|^2}{2\sigma^2}} \cdot t^{\frac{d}{2}-1} e^{-\frac{1}{2}t} \mathcal{I}_d(\sigma^{-1}|n|\sqrt{t}), \quad (t \geq 0), \quad (1.8)$$

where $|n|$ denotes the Euclidean norm of n in \mathbb{R}^d and

$$\mathcal{I}_d(u) = \frac{1}{2 \cdot (2\pi)^{d/2}} \int_{\mathbb{S}^{d-1}} e^{u\langle \omega, e_1 \rangle} d\omega,$$

with e_1 being the first standard co-ordinate vector in \mathbb{R}^d and $d\omega$ being the standard spherical measure on \mathbb{S}^{d-1} .

Remark 1.3. For $d = 2$, the function \mathcal{I}_d turns out to be closely related to the modified Bessel function of the first kind, given by (cf. [40])

$$I_0(z) = \frac{1}{2\pi} \int_0^{2\pi} e^{z \cos \varphi} d\varphi, \quad (\operatorname{Re} z > 0).$$

For general d , it is easy to see that

$$\mathcal{I}_d(u) = \frac{1}{2^{d/2} \pi^{1/2} \Gamma(\frac{d-1}{2})} \int_0^\pi e^{u \cos \varphi} (\sin \varphi)^{d-2} d\varphi. \quad (1.9)$$

Then we can state

Theorem 1.4. (i) The coverage probability is given by

$$p_c(\theta, \beta, \sigma) = \sum_{n \in \Lambda} \int_0^\infty \left\{ \prod_{j \neq n \in \Lambda} \int_t^\infty \left(1 + \theta \frac{t^{d\beta/2}}{u^{d\beta/2}} \right)^{-1} f(u, j, \sigma) du \right\} f(t, n, \sigma) dt. \quad (1.10)$$

(ii) The limit $C_1(\beta, \sigma) = \lim_{\theta \rightarrow \infty} \theta^{\frac{1}{\beta}} p_c(\theta, \beta, \sigma)$ exists and

$$C_1(\beta, \sigma) = \sum_{n \in \Lambda} e^{-\frac{|n|^2}{\sigma^2}} \int_0^\infty \left\{ \prod_{j \neq n \in \Lambda} \int_0^\infty \left(1 + \frac{s^{d\beta/2}}{u^{d\beta/2}} \right)^{-1} f(u, j, \sigma) du \right\} \frac{s^{\frac{d}{2}-1}}{2^{d/2} \Gamma(d/2)} ds.$$

A key implication of Theorem 1.4 is that, for fixed β and σ , the curve $p_c(\theta, \beta, \sigma)$ v.s. θ is asymptotically a power law, and therefore, for large values of θ , improving the coverage probability amounts to designing networks that provide a bigger value for $C_1(\beta, \sigma)$, which is purely a lattice-dependent quantity for a given level of disorder σ .

We defer the proof of Theorem 1.4, along with the statement and proof of an auxiliary lemma, to Section 8.1.

1.5 Main results and contributions

Herein, we discuss the main results and contributions obtained in this paper.

Disordered lattices as spatial random network models. A central theme in this work is to demonstrate that disordered lattice models (i.e. network models based on random perturbations of Euclidean lattices) as highly effective models for random spatial networks, covering in particular applications to wireless network models. We demonstrate that disordered lattices interpolate between Poisson and Ginibre networks, and allow us to achieve the best of both worlds : significantly improve upon the Poisson model in terms of network efficacy measured by the SINR, at the same time retaining a considerable measure of mathematical and computational simplicity and robustness to erasure and noise. Our approach is substantiated via theoretical analysis as well as empirical investigations. Detailed comparisons of performance to Poissonian and Ginibre networks are carried out in Section 5. Furthermore, we prescribe the optimal lattice and the optimal level of disorder for perturbed lattice models in the context of wireless network

applications. These are explored in detail in Sections 3 and 5 respectively. The closest approximation to a Ginibre point process by a disordered lattice model is obtained at the disorder level $\sigma \sim 0.4$, which interestingly is also the disorder level at which the coverage probability distributions of the two network models roughly match. In a nutshell, we put forward disordered lattice models as a viable paradigm to answer the questions alluded to in the three-fold investigative framework of Section 1.2.

Coverage probability for disordered lattice and power-law asymptotics. We obtain an explicit expression for the coverage probability for a general disordered lattice which, albeit in the form of an infinite sum of infinite products, provides a non-random object that can be investigated numerically. In fact, it is explicit enough to demonstrate that, in the regime of large threshold θ , the coverage probability is asymptotically a power law. This is considered in Theorem 1.4.

Optimal lattices and connections to the Epstein Zeta function. We connect our search for optimal lattices in the context of perturbed lattice models to the celebrated Epstein Zeta function of a lattice, a kind of lattice energy that is of intrinsic interest in number theory and other branches of pure mathematics. This is taken up for detailed consideration in Section 3. In summary, our theoretical investigations suggest that the behaviour of SINR (and coverage probabilities) is optimised by considering perturbations of lattices that minimize the Epstein Zeta function. In 2D, this leads to the choice of the triangular lattice, whereas in 3D this suggests considering the face centred cubic (abbrev. FCC) lattice.

Theoretical analysis of SINR in extremal regimes. In wireless networks, the SINR is an object of central importance; in the setting of disordered networks it is a random variable. The SINR is notoriously difficult to handle theoretically, evading a neat mathematical description, which makes its theoretical analysis complicated. However, in this work, we obtain an approximate theoretical understanding of the SINR in certain settings, focussing on regimes of small (or large) parameters, which has important implications for wireless networks (Section 2). In particular, such understanding motivates our considerations for optimal lattice.

In the regime of small σ , we are able to obtain an approximation of the coverage function near a base station by a log-normal random variable with explicitly specified parameters (Section 2.2). This leads to an approximation of the coverage probability by an explicit closed form integral that is at the same time simple enough to be numerically tractable.

In the regime of small σ and large θ , we carry out further theoretical analysis that suggests explicit parametric dependencies of the coverage probability (c.f. Theorem 1.4) in this regime (Section 2.3). Notably, our studies indicate an inverse dependence on σ (in the form of an explicit power law) - an effect that is corroborated by our empirical investigations in Section 5. It also suggests an inverse (power-law) dependence on the Epstein Zeta function of the lattice, lending further credence to our choice of optimal lattice via a comparison of lattice energies.

In the regime of small σ and small θ , we unveil an approximation that entails linear dependence of the coverage probability near a base station on θ , and demonstrates worsening behaviour with increase in σ . Finally, our theoretical studies of the SINR indicate its monotonicity in σ in the small σ regime.

A paradigm for measuring proximity between point sets. In this work, we unveil a paradigm for measuring the proximity between point sets, which we believe would be of independent interest in a wide range of applications. Our approach considers the so-called *Persistence Diagrams* of the point sets, and computes the *Total Variation* distance between these (also exploring alternative possibilities such as the *symmetrised nearest neighbour distance*). As elaborated in Section 4.1, the persistence diagram effectively captures the higher order geometry of a point set, making it a comprehensive and robust observable for this purpose.

It turns out (reference) that the closest approximation to a Ginibre random point set by a Perturbed Triangular Lattice in 2D is obtained near the disorder value $\sigma = 0.4$, which is interestingly also the disorder level at which the SINR for this lattice model closely approximates (and slightly outperforms) the SINR for the Ginibre model. This enables us to suggest that a perturbed triangular lattice with disorder level $\sigma = 0.4$ is an appropriate substitute for the Ginibre random network, while having the additional advantages of simplicity and robustness that are accorded by a disordered lattice model.

We complement our investigations on measuring proximity between point sets by a much simpler observable to understand the geometry of a point set, which is via its *Nearest Neighbour Distribution*. Measuring distances between the nearest neighbour distance curves, while much cruder and less comprehensive than via their persistence diagrams, can nevertheless be considered in situations where computation simplicity is a greater consideration than accuracy.

Disordered lattice models interpolating with Poissonian networks. We complete our investigations by rigorously demonstrating that disordered lattice networks interpolate lattices with Poissonian networks. This is entailed by a convergence of disordered lattices to the Poisson point process as random point configuration. In fact, we are able to demonstrate a result that holds in much greater generality; this is captured by Theorem 6.1 in Section 6. The proof of Theorem 6.1 invokes classical theory of diffusions on infinite particle systems. This convergence is further borne out empirically by the convergence of the nearest neighbour distributions of the disordered lattice models to that of the Poissonian network (c.f. Fig. 10 and Fig. 11).

Comparison with Poissonian network. The crucial comparison between disordered lattice networks and the popularly used Poissonian network is that of the coverage probability distributions. It is demonstrated via our empirical investigations in Section 5 that for all values of disorder considered, the coverage probability for the disordered lattice has a better behaviour than Poisson at the same threshold θ . This is indicated by the a higher value of the coverage function for the disordered lattices, which entails that the coverage function curve for those lie above that of the Poisson network (c.f. Fig. 4 and Fig. 6).

2 SINR in extremal parameter regimes

2.1 The regime of small σ : generalities

In this section, we will examine the approximate behaviour of the coverage probability in the small σ regime, and explore the various consequences thereof in subsequent sections. We focus on the setting where the configuration Φ of base stations is a perturbation of the lattice Λ by the i.i.d. random variables $\{\sigma\xi_\lambda\}_{\lambda\in\Lambda}$, with ξ_λ being i.i.d. on \mathbb{R}^d with unit standard deviation and $\sigma > 0$ being the common standard error of the perturbations. For $\lambda \in \Lambda$, set $X_\lambda = \lambda + \sigma\xi_\lambda$.

For a point configuration $\Phi = \sum_{i=1}^\infty \delta_{X_i}$ and a given threshold $\theta > 0$, we will consider the coverage function at the location a , given by

$$\mathcal{C}(\Phi; a) := \prod_{\lambda \neq B} \left(1 + \theta \frac{|X_B - a|^{d\beta}}{|X_\lambda - a|^{d\beta}} \right)^{-1}, \quad (2.1)$$

where λ ranges over Λ except B . This is in fact the coverage probability for given locations of the base stations (the randomness being in the fading), which is called the meta-distribution of SINR ([31]). In subsequent discussions, for a point configuration Λ and a point $\mathbf{a} \in \Lambda$, we will denote by $\Lambda_{\mathbf{b}}$ the point configuration consisting of all points of Λ except \mathbf{b} .

In Section 1.4 we considered translation invariant point processes as base station configurations. This would imply that the statistical distribution of the SINR is the same at all points of space, and therefore it suffices to consider the SINR at the origin. Here, we consider an equivalent way of describing the same random variable. To this end, we let Δ to a *primitive unit cell* of the lattice containing the origin; e.g. for a triangular lattice in \mathbb{R}^2 , it is an equilateral triangle with side length equalling the lattice spacing having the origin as a vertex. Let $U(\Delta)$ denote the uniform distribution on Δ . Let Φ be a perturbation of the lattice Λ as above, and let $\bar{\Phi}$ be the translation invariant version of Φ . For a point process Φ on \mathbb{R}^d and a location $p \in \mathbb{R}^d$, we use $\text{SINR}_p(\Phi)$ to denote the random variable that is the SINR at p for a base station configuration sampled from the process Φ .

With these notations, if $\mathbf{x} \sim U(\Delta)$ and statistically independent of Φ , then the random variables $\text{SINR}_o(\bar{\Phi})$ and $\text{SINR}_{\mathbf{x}}(\Phi)$ have the same statistical distribution. Thus, in order to understand $\text{SINR}_o(\bar{\Phi})$, it is of interest to study the the random coverage function $\mathcal{C}(\Phi; \mathbf{x})$, in view of Proposition 1.1.

In the regime of small σ , with high probability the nearest base station to \mathbf{x} will be the lattice perturbation of the one of the vertices of Δ ; we denote the latter by B . We recall from (2.1) that

$$\begin{aligned} \mathcal{C}(\Phi; \mathbf{x}) &:= \prod_{\lambda \neq B} \left(1 + \theta \frac{|X_B - \mathbf{x}|^{d\beta}}{|X_\lambda - \mathbf{x}|^{d\beta}} \right)^{-1} \\ &= \prod_{\lambda \neq B} \left(1 + \theta \frac{|B + \xi_B - \mathbf{x}|^{d\beta}}{|\lambda + \xi_\lambda - \mathbf{x}|^{d\beta}} \right)^{-1}. \end{aligned}$$

Notice that $\mathbf{x} - B$ is also uniformly distributed on a primitive unit cell of the lattice, and has the origin as the nearest lattice point. In view of this, we may focus attention to the case $B = \mathbf{0}$, the origin in \mathbb{R}^d . Thus, we are interested in the random variable

$$\prod_{\lambda \neq \mathbf{0}} \left(1 + \theta \frac{|X_{\mathbf{0}} - \mathbf{x}|^{d\beta}}{|X_\lambda - \mathbf{x}|^{d\beta}} \right)^{-1} = \prod_{\lambda \neq \mathbf{0}} \left(1 + \theta \frac{|\sigma \xi_{\mathbf{0}} - \mathbf{x}|^{d\beta}}{|(\lambda - \mathbf{x}) + \sigma \xi_\lambda|^{d\beta}} \right)^{-1} \quad (2.2)$$

on the event that the closest lattice point to \mathbf{x} is the origin $\mathbf{0}$.

Observe that since \mathbf{x} is constrained to be closer to $\mathbf{0}$ than other vertices of Δ in (2.2), there is an automatic bound on $|\mathbf{x}|$ that places it close to the origin. A rich statistical behaviour arises, however, when \mathbf{x} is further constrained to be at the origin. In the interest of brevity, we focus on this detailed statistical structure in the present paper, postponing a more comprehensive analysis of the situation with general \mathbf{x} for future work. In other words, in the rest of this section, we will focus on

$$\mathcal{C}_0(\Phi) := \prod_{\lambda \neq \mathbf{0}} \left(1 + \theta \frac{|\sigma \xi_{\mathbf{0}}|^{d\beta}}{|\lambda + \sigma \xi_{\lambda}|^{d\beta}} \right)^{-1} \quad (2.3)$$

As we shall see, the statistical structure of $\mathcal{C}_0(\Phi)$ already suggests natural choices for the lattice Λ in 2 and 3 dimensions, which are the settings of greatest practical significance. From a modelling perspective, the focus on $\mathbf{x} = \mathbf{0}$ can be envisaged as a situation where we have a specially important point of interest (viz., the origin) and we intend to put a base station near that location, and want to focus attention on the SINR at that special point in the presence of the confounding effect of interference from farther base stations and ambient noise.

Remark 2.1. It may be noted that, although we are focussing at the origin in this section for a detailed statistical examination of the SINR, the comparison of different point fields in this paper, such as in Section 5 are all with regard to the standard definition of SINR_o where the translation invariance of the point process has been taken into account. The discussions in this section are envisaged as an exploration of some broad structural features of the perturbed lattice models as network distributions, rather than as rigorous theorems which would establish certain expected phenomena.

2.2 The regime of small σ : a log-normal approximation

We examine the logarithm of the coverage function near a base station

$$\log \mathcal{C}_0(\Phi) = - \sum_{\lambda \in \Lambda_{\mathbf{0}}} \log \left(1 + \theta \frac{|\sigma \xi_{\mathbf{0}}|^{d\beta}}{|\lambda + \sigma \xi_{\lambda}|^{d\beta}} \right) = - \sum_{\lambda \in \Lambda_{\mathbf{0}}} \log \left(1 + \theta \sigma^{d\beta} \frac{|\xi_{\mathbf{0}}|^{d\beta}}{|\lambda + \sigma \xi_{\lambda}|^{d\beta}} \right).$$

Since $\lambda \neq \mathbf{0}$ and we are in the small σ regime, we may expand the logarithm in a series as

$$\log \left(1 + \theta \sigma^{d\beta} \frac{|\xi_{\mathbf{0}}|^{d\beta}}{|\lambda + \sigma \xi_{\lambda}|^{d\beta}} \right) = \sum_{k=1}^{\infty} \frac{(-1)^{k+1}}{k} \theta^k \sigma^{d\beta k} \frac{|\xi_{\mathbf{0}}|^{d\beta k}}{|\lambda + \sigma \xi_{\lambda}|^{d\beta k}}.$$

Therefore, we have for $\log \mathcal{C}_0(\Phi)$ the expansion

$$\log \mathcal{C}_0(\Phi) = \sum_{k=1}^{\infty} \frac{(-1)^k}{k} \theta^k \sigma^{d\beta k} \left(\sum_{\lambda \in \Lambda_{\mathbf{0}}} \frac{|\xi_{\mathbf{0}}|^{d\beta k}}{|\lambda + \sigma \xi_{\lambda}|^{d\beta k}} \right). \quad (2.4)$$

As $\sigma \rightarrow 0$, the terms in the above expansion decay exponentially fast in k , so to the leading order in σ we get

$$\log \mathcal{C}_0(\Phi) = -\theta \sigma^{d\beta} \left(\sum_{\lambda \in \Lambda_{\mathbf{0}}} \frac{|\xi_{\mathbf{0}}|^{d\beta}}{|\lambda + \sigma \xi_{\lambda}|^{d\beta}} \right) + O(\sigma^{2d\beta}). \quad (2.5)$$

Observe that

$$|\lambda + \sigma \xi_{\lambda}|^{-d\beta} = |\lambda|^{-d\beta} \left| \omega_{\lambda} + \sigma \frac{\xi_{\lambda}}{|\lambda|} \right|^{-d\beta}, \quad (2.6)$$

where ω_{λ} is the direction of the vector $\lambda \in \Lambda$ (so that ω_{λ} is an element of \mathbb{S}^{d-1}).

Then, in the small σ regime, we can expand

$$\begin{aligned} \left| \omega_{\lambda} + \sigma \frac{\xi_{\lambda}}{|\lambda|} \right|^{-d\beta} &= \left(1 + 2\sigma \frac{\langle \omega_{\lambda}, \xi_{\lambda} \rangle}{|\lambda|} + \sigma^2 \frac{|\xi_{\lambda}|^2}{|\lambda|^2} \right)^{-\frac{1}{2}d\beta} \\ &= 1 - d\sigma \beta \frac{\langle \omega_{\lambda}, \xi_{\lambda} \rangle}{|\lambda|} + O(\sigma^2). \end{aligned}$$

Combined with (2.5) and (2.6), this implies that, to the leading order in σ we have

$$\log \mathcal{C}_0(\Phi) = -\theta \sigma^{d\beta} |\xi_{\mathbf{0}}|^{d\beta} \left[\sum_{\lambda \in \Lambda_{\mathbf{0}}} \left(\frac{1}{|\lambda|^{d\beta}} - d\sigma \beta \frac{\langle \omega_{\lambda}, \xi_{\lambda} \rangle}{|\lambda|^{d\beta+1}} \right) \right] + O(\sigma^{d\beta+2}).$$

At this point, we recall the Epstein Zeta function of the lattice Λ (at the parameter s) as

$$\mathcal{E}_{\Lambda}(s) = \sum_{\lambda \in \Lambda_{\mathbf{0}}} \frac{1}{|\lambda|^s}, \quad (2.7)$$

see, e.g., ([57, 56]). Using the Epstein Zeta function, we can express the leading order behaviour of the log coverage function near a base station as

$$\log \mathcal{C}_0(\Phi) = -\theta \sigma^{d\beta} |\xi_0|^{d\beta} \mathcal{E}_\Lambda(d\beta) + d\theta \beta \sigma^{d\beta+1} |\xi_0|^{d\beta} \left(\sum_{\lambda \in \Lambda_0} \frac{\langle \omega_\lambda, \xi_\lambda \rangle}{|\lambda|^{d\beta+1}} \right) + O(\sigma^{d\beta+2}). \quad (2.8)$$

We now focus on the situation where, for a given location of the nearest base station, we are interested in the behaviour of the coverage function near a base station as the locations of the other base stations and the fading fluctuates randomly. In other words, we fix the *signal*, and investigate the statistical effects of the *interference* on the coverage probability. From the analysis presented above, it is clear that for a given location of the nearest base station ξ_0 and small σ , the coverage function near a base station $\mathcal{C}_0(\Phi)$ (equivalently, its logarithm) is maximised when $\mathcal{E}_\Lambda(d\beta)$ is minimised. This is the famous problem of finding the minimizing lattice for the Epstein Zeta function ([50]).

To make further analysis, we focus on the natural setting of the perturbations $\{\xi_\lambda\}_{\lambda \in \Lambda}$ being d -dimensional standard Gaussians. It may be noted that, if ξ_λ is a d -dimensional standard Gaussian, then $\eta_\lambda := \langle \omega_\lambda, \xi_\lambda \rangle$ is a 1-dimensional Gaussian with mean 0 and variance 1. As a result, it may be deduced that the random sum

$$\left(\sum_{\lambda \in \Lambda_0} \frac{\langle \omega_\lambda, \xi_\lambda \rangle}{|\lambda|^{d\beta+1}} \right)$$

is in fact a 1-dimensional Gaussian with mean 0 and variance $\mathcal{E}_\Lambda(2d\beta + 2)$.

This implies that in the regime of small σ , the coverage function near a base station $\mathcal{C}_0(\Phi)$, for any given location ξ_0 of the nearest base station, is approximately a log-normal random variable (cf. [36]) with parameters

$$-\theta \sigma^{d\beta} |\xi_0|^{d\beta} \mathcal{E}_\Lambda(d\beta) \quad \text{and} \quad \theta \beta \sigma^{d\beta+1} |\xi_0|^{d\beta} \sqrt{\mathcal{E}_\Lambda(2d\beta + 2)}. \quad (2.9)$$

For practical purposes (e.g., for using Monte Carlo methods to study the coverage probabilities, guaranteeing a high coverage probability against the randomness of the fading and the environment, etc.), it would also be of interest to work with a lattice Λ such that the coverage function near a base station (equivalently, its logarithm) is the most *stable*. This would amount to the choice of a lattice so as to minimize the fluctuations or the variance

of $\log \mathcal{C}_0(\Phi)$. Once again, for a given nearest base station ξ_0 , this amounts to choosing a lattice that minimizes the Epstein Zeta function $\mathcal{E}_\Lambda(2d\beta + 2)$. The minimizing lattice for this in 2D is the triangular lattice, and in 3D, for our regime of interest $\beta > 1$, the minimizing lattice is conjectured to be the FCC.

We now examine the coverage probability itself, which, in view of the analysis presented above, would amount to considering the expectation of a log-normal random variable with parameters as specified in (2.9) (conditioned on ξ_0), with $|\xi_0|$ following a d -dimensional standard Gaussian distribution.

We first condition on ξ_0 and obtain the expectation of the log-normal as

$$\exp \left(-\theta \sigma^{d\beta} |\xi_0|^{d\beta} \mathcal{E}_\Lambda(d\beta) + \frac{1}{2} \theta^2 \beta^2 \sigma^{2d\beta+2} |\xi_0|^{2d\beta} \mathcal{E}_\Lambda(2d\beta + 2) \right).$$

In the small σ -regime, we may approximate the exponent in this quantity by the leading term in σ . We can then take expectation with respect to ξ_0 following a d -dimensional standard Gaussian distribution to obtain the final coverage probability.

Thus, the coverage probability can be approximated, in the small σ regime, by

$$\mathbb{E}_{\xi_0 \sim N(\mathbf{0}, I_d)} \left[\exp \left(-\theta \sigma^{d\beta} |\xi_0|^{d\beta} \mathcal{E}_\Lambda(d\beta) \right) \right].$$

We then observe that, if $\xi_0 \sim N(\mathbf{0}, I_d)$, then $|\xi_0|^2 \sim \chi_d^2$, that is, the Chi-squared distribution with d degrees of freedom. The probability density function for the χ_d^2 distribution on positive reals can be expressed as ([36])

$$f_{\chi_d^2}(x) = \frac{1}{2^{d/2} \Gamma(d/2)} x^{d/2-1} e^{-x/2}, \quad (2.10)$$

where $\Gamma(\alpha)$ is the Gamma integral given by $\int_0^\infty x^{\alpha-1} e^{-x} dx$. We can therefore write the coverage probability above as

$$\frac{1}{2^{d/2} \Gamma(d/2)} \int_0^\infty u^{d/2-1} \exp \left(-\theta \sigma^{d\beta} \mathcal{E}_\Lambda(d\beta) u^{\frac{1}{2}d\beta} - \frac{1}{2} u \right) du. \quad (2.11)$$

2.3 The regime of small σ and large θ : parametric dependencies of coverage probability

In this section, we explore the asymptotics (for large θ) in the coverage probability near a base station, via the asymptotics of the integral (2.11).

The asymptotics of (2.11) below indicate a power law scaling as $\theta^{-1/\beta}$. In the context of Theorem 1.4 (which also exhibits a similar $\theta^{-1/\beta}$ scaling), the leading constant $C_2(\beta, \sigma)$ in the asymptotics of (2.11) is analogous to the leading constant $C_1(\beta, \sigma)$ in that theorem. The simpler algebraic structure of $C_2(\beta, \sigma)$, however, unveils a clear power law dependency on σ , which suggests a similar σ -dependency for the limiting constant $C_1(\beta, \sigma)$. In our considerations of this asymptotic, we consider σ to be small but fixed, and $\theta \rightarrow \infty$. It would be of interest to extend such suggestive behaviour to obtain a theorem that rigorously proves a comprehensive dependency structure for $C_1(\beta, \sigma)$; for reasons of brevity we leave that question for future research.

In the regime of large θ and small σ , since $\beta > 1$, the integral (2.11) is approximately

$$\frac{1}{2^{d/2}\Gamma(d/2)} \int_0^\infty u^{d/2-1} \exp\left(-\theta\sigma^{d\beta}\mathcal{E}_\Lambda(d\beta)u^{\frac{1}{2}d\beta}\right) du.$$

Setting $v = u^{\frac{1}{2}d\beta}$ and $a = \theta\sigma^{d\beta}\mathcal{E}_\Lambda(d\beta)$ in the above, we reduce the integral to

$$\begin{aligned} \frac{1}{2^{d/2}\Gamma(d/2)} \frac{2}{d\beta} \int_0^\infty v^{\frac{1}{\beta}-1} e^{-av} dv &= \frac{1}{2^{d/2-1}\Gamma(d/2)} \frac{\Gamma(1/\beta)}{d\beta} a^{-1/\beta} \\ &= \frac{\Gamma(1/\beta)}{d\beta 2^{d/2-1}\Gamma(d/2)\mathcal{E}_\Lambda(d\beta)^{1/\beta}\sigma^d} \cdot \theta^{-1/\beta} \\ &= C_2(\beta, \sigma) \cdot \theta^{-1/\beta}, \end{aligned} \tag{2.12}$$

where

$$C_2(\beta, \sigma) = \frac{\Gamma(1/\beta)}{d\beta 2^{d/2-1}\Gamma(d/2)\mathcal{E}_\Lambda(d\beta)^{1/\beta}} \cdot \sigma^{-d}.$$

Therefore, in the small σ regime, (2.12) recovers the large θ asymptotics of the coverage probability near a base station as $\theta^{-1/\beta}$, and suggests a parametric dependency of the limiting constant $C_1(\beta, \sigma)$ (c.f. Theorem 1.4) as an inverse power law in σ as $\Gamma(1/\beta) \cdot (d\beta 2^{d/2-1}\Gamma(d/2)\mathcal{E}_\Lambda(d\beta)^{1/\beta})^{-1} \cdot \sigma^{-d}$. Such parametric dependence on σ is corroborated empirically by Figs. 3 – 6.

2.4 The regime of small σ and small θ : asymptotic linearity

The regime of small θ is important in the wireless network model for the following reason. We are able to detect a signal as soon as the SINR is above

some threshold, that is, the SINR is not too low. From this perspective, it would be relevant to have $\mathbb{P}[\text{SINR}_o > \theta]$ to be high for small values of θ , with the pertinent question being its dependence on θ as $\theta \rightarrow 0$. Accordingly, we obtain an approximation of the coverage probability in the regime of small θ and σ .

In the integral (2.11), we can approximate $\exp\left(-\theta\sigma^{d\beta}\mathcal{E}_\Lambda(d\beta)u^{\frac{1}{2}d\beta}\right)$ by $\left(1 - \theta\sigma^{d\beta}\mathcal{E}_\Lambda(d\beta)u^{\frac{1}{2}d\beta}\right)$ in the regime of small θ , and therefore obtain an approximation for the coverage probability near a base station as

$$\begin{aligned} & 1 - \theta\sigma^{d\beta}\mathcal{E}_\Lambda(d\beta)\frac{1}{2^{d/2}\Gamma(d/2)}\int_0^\infty u^{d/2-1}u^{\frac{1}{2}d\beta}e^{-\frac{1}{2}u}du \\ &= 1 - \theta\sigma^{d\beta}\mathcal{E}_\Lambda(d\beta)\frac{2^{\frac{1}{2}d(\beta+1)}\Gamma(\frac{1}{2}d(\beta+1))}{2^{d/2}\Gamma(d/2)} \\ &= 1 - 2^{\frac{1}{2}d\beta}\sigma^{d\beta}\mathcal{E}_\Lambda(d\beta)\frac{\Gamma(\frac{1}{2}d(\beta+1))}{\Gamma(\frac{1}{2}d)} \cdot \theta. \end{aligned} \quad (2.13)$$

Thus, in the small θ regime, the coverage probability near a base station decays approximately linearly in θ , with the slope being given by (2.13). We once again observe a worsening behaviour of the coverage probability with increasing σ .

2.5 Monotonicity in σ

In this section, we will demonstrate that, in the regime of small σ , the coverage probability near a base station for Gaussian perturbed lattice networks, for a given threshold θ , is monotonically decreasing in the dispersion σ of the perturbation.

To this end, we will consider the coverage function near a base station $\mathcal{C}_0(\Phi, \sigma)$:

$$\begin{aligned} \log \mathcal{C}_0(\Phi, \sigma) &= - \sum_{\lambda \in \Lambda_0} \log \left(1 + \theta \frac{|\sigma \xi_0|^{d\beta}}{|\lambda + \sigma \xi_\lambda|^{d\beta}} \right) \\ &= - \sum_{\lambda \in \Lambda_0} \log \left(1 + \theta |\xi_0|^{d\beta} \frac{1}{\left| \frac{1}{\sigma} \lambda + \xi_\lambda \right|^{d\beta}} \right). \end{aligned}$$

The derivative of $\log \mathcal{C}_0(\Phi, \sigma)$ with respect to σ is given by

$$\begin{aligned} & \frac{\partial}{\partial \sigma} \log \mathcal{C}_0(\Phi, \sigma) \\ &= - \sum_{\lambda \in \Lambda_0} \left(1 + \theta |\xi_0|^{d\beta} \frac{1}{|\frac{1}{\sigma}\lambda + \xi_\lambda|^{d\beta}} \right)^{-1} \frac{-\beta \theta |\xi_0|^{d\beta}}{|\frac{1}{\sigma}\lambda + \xi_\lambda|^{d\beta+2}} \frac{\partial}{\partial \sigma} \left[\left| \frac{1}{\sigma}\lambda + \xi_\lambda \right|^2 \right] \end{aligned} \quad (2.14)$$

and

$$\begin{aligned} \frac{\partial}{\partial \sigma} \left[\left| \frac{1}{\sigma}\lambda + \xi_\lambda \right|^2 \right] &= 2 \left\langle \frac{1}{\sigma}\lambda + \xi_\lambda, \frac{-1}{\sigma^2}\lambda \right\rangle \\ &= -2 \left(\frac{|\lambda|^2}{\sigma^3} + \frac{\langle \xi_\lambda, \lambda \rangle}{\sigma^2} \right) \\ &= -2 \frac{|\lambda|^2}{\sigma^3} \left(1 + \sigma \cdot \frac{\langle \omega_\lambda, \xi_\lambda \rangle}{|\lambda|} \right), \end{aligned}$$

where $\omega_\lambda \in \mathbb{S}^{d-1}$ in the direction of the vector $\lambda \in \mathbb{R}^d$, as before.

In the small σ regime, with high probability $\left| \sigma \cdot \frac{\langle \omega_\lambda, \xi_\lambda \rangle}{|\lambda|} \right| \ll 1$ for all non-zero $\lambda \in \Lambda_0$, which, in light of (2.14), implies that the logarithmic derivative $\frac{\partial}{\partial \sigma} \log \mathcal{C}_0(\Phi, \sigma)$ is negative.

Thus, in the small σ regime, the coverage function near a base station is, with high probability, monotonically decreasing in σ . Since the coverage probability is the expectation of the coverage function, this indicates in the small σ regime, the coverage probability near a base station would decrease with increasing σ .

3 Choice of lattice and energy optimality

An important question that arises in studying disordered lattices as models for wireless base stations is the choice of the lattice which we perturb. In this direction, we are guided by considerations of energy optimality of lattices, which appears rather interestingly in our investigations of the coverage probability.

To be more precise, we can consider Gaussian perturbations of a lattice Λ with dispersion parameter σ . The coverage probability curve is then a

function of σ . Although this function is not analytically tractable, we can nevertheless expand it in a series in σ in the regime where the parameter σ is small, as we demonstrate in Section 2.2. The coefficients of this expansion, naturally, are functionals of the lattice Λ .

It turns out, as in (2.8), that the coefficient of the leading term in this expansion is the celebrated Epstein Zeta Function of the lattice Λ , which, heuristically speaking, can be thought of as a lattice energy, and has deep connections to sphere packing, number theory, crystallography, quantum field theory and other diverse areas of mathematics and physics (see, e.g., [57, 56, 22, 12]). Maximizing the coverage probability at a given level θ would amount to considering the lattice that minimizes the Epstein Zeta Function, a classical problem in its own right, that has connections to other fundamental questions like the crystallisation conjecture ([50, 8, 18, 6, 51, 49, 30]). In 2D Euclidean space, the minimizing lattice for the Epstein Zeta function is the triangular lattice, which is the focus of our attention. In 3D Euclidean space, a rigorous understanding of minimal lattices for the Epstein Zeta function is limited, but, as we argue in Section 5.2, a natural choice to focus on is the Face Centered Cubic (FCC) lattice and its Gaussian perturbation (i.e., the perturbed FCC (abbrv. PFCC)).

4 Comparison of random point sets and persistent homology

4.1 Comparison via persistent diagrams

One of the issues that we address in our investigations is the comparison between point processes that are candidates for modelling the locations of the wireless base stations. An interesting question on its own right, this is also motivated by the desire to find disordered lattices which are appropriate “substitutes” for the random matrix networks - in particular, this entails a comparison between the two point processes. To compare two point configurations, we appeal to their *persistence diagrams* (abbrv. PDs), a tool that has recently attracted a lot of interest in topological data analysis. For details on persistence diagrams and random topology, we refer the reader to recent articles ([21, 61, 65, 33]), to provide a partial list. In the limited scope available to us here, we give a succinct heuristic description as follows, with concrete definitions in Appendix A.

We can consider random geometric graphs on a point set by connecting pairs of points by an edge when they are nearer than a given threshold ε , and more generally form a k -clique out of k points if the ε balls around these k points intersect pairwise. As ε varies from 0 to ∞ , more points get connected with each other. The topological properties of the point set can be discussed in terms of *homology groups* related to certain *complexes* arising out of this construction.

Heuristically speaking, such considerations entail that the fundamental topological properties of the point set are captured by certain *holes* embedded in the point set fattened by the ε -balls. Holes appear and disappear (due to the overlap of the balls around the points) as the connectivity threshold ε changes. The most significant ones among these holes are those that *persist* for a long time, that is, the thresholds for their appearance and disappearance are well-separated. Morally, such *persistent* holes reflect a fundamental feature of the point set compared to less persistent ones, whose appearance could be attributed to random noise. The PD corresponding to the point set is a 2D plot against each other of these two thresholds (resp. for appearance and disappearance) for these holes.

We compare two point configurations by comparing their persistence diagrams, which brings us to the natural question of comparing two persistence diagrams. To this end, we adopt two approaches.

For the first approach, we consider the persistence diagrams as atomic probability measures. We then proceed to compute the *Total Variation distance* (abbrv. TV distance) between these two measures. For two probability measures having densities f and g on the same Euclidean space, it can be expressed simply as the integral $\int |f(x) - g(x)|dx$. For computational simplicity, we convolve the atomic measures given by the PDs with Gaussians having a small dispersion (equal to $1/2$) and discount the contribution from atoms near diagonal of the PD (cf. [39]), and take the TV distance between the resulting measures with densities via the above formula.

For the second approach, we make use of the fact that PDs themselves are 2D finite point sets, and we compute the *distance* between two PDs by computing their *symmetrized nearest-point distance* ([42]). In particular, let X, Y be two finite point configurations in a metric space (equipped with the metric d), and for $x \in X$, let $y(x)$ be the nearest point to x in Y (making arbitrary choices to break ties, if any). Then define a distance between the configurations X, Y as $\bar{d}(X, Y) = \sum_{x \in X} d(x, y(x))$. Now $\bar{d}(\cdot, \cdot)$ is clearly asymmetric in its arguments, so we define the symmetrized nearest-point

distance between X and Y as $D(X, Y) = \bar{d}(X, Y) + \bar{d}(Y, X)$.

We mention in passing that other metrics for measuring distance between PDs have been considered, e.g. the *bottleneck distance* ([13]). However, the calculation of such metrics on given data sets can often be highly computationally intensive. In this article, we focus on the total variation and symmetrized nearest-point distances for their simplicity and computational tractability. The comparative study of wireless network distributions (and more generally, point processes) with respect to other metrics on PDs certainly warrant further investigation; though, as exemplified by the consistency of the minimality threshold of around $\sigma = 0.4$ across our chosen metrics in this paper, we expect our broad conclusions to be more or less robust to the specifics of the metrics involved.

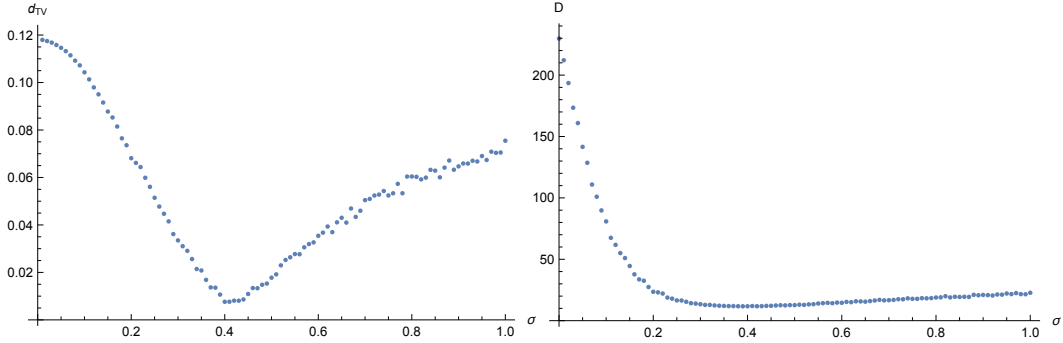


Figure 2: Distance between Persistence Diagrams of Ginibre and PTL point processes. Left panel: Total Variation distance between the PDs considered as point measures. Right panel: $D(\cdot, \cdot)$ distance between the PDs. Around $\sigma = 0.4$, the PDs are the closest in both metrics.

It may be noted that PDs of random point sets are random 2D point sets themselves. So, eventually we are comparing another pair of (random) point sets rather than the original point processes directly. However, the comparison of PDs enjoys two advantages over a direct comparison of the point processes.

First, the PDs are always 2D point sets located on the same domain (the positive quadrant in \mathbb{R}^2). As such, their comparison via the metric \bar{d} is always reasonable, irrespective of the nature of the ambient spaces in which the original point processes are embedded (e.g., this allows for the comparison of point processes that are embedded in Euclidean spaces of different dimensions). Thus, the comparison of PDs truly focuses on a desirable comparison

of the structural properties of the point set and is oblivious to extraneous factors like its physical embedding.

Secondly, passing from the original point process to the PD controls the influence of outliers, and consequently has a stabilizing effect with respect to random noise, which is better for comparison purposes.

4.2 Comparison via nearest neighbour distribution

An important aspect of point patterns is their nearest neighbour distribution (abbrv. *nnd*), that is, the statistical distribution of the typical point from its nearest neighbour. A renowned instance of this is the 1D case, where this reduces to the famous level spacing distribution that has been widely investigated in the context of random matrix theory ([43]). A significant result in this direction, that traces its origin as far back as Wigner’s work, is that the level spacing distributions of Gaussian random matrix ensembles are very different from, say, the *independent case* (i.e., the Poisson point process), and a great volume of research has been dedicated to successfully establishing the conjecture that such behaviour is, in fact, *universal* (i.e., not dependent on the Gaussianity or other specifics of the matrix distributions) (see, e.g., [25, 55]). In particular, the repulsion among the points in the Ginibre ensembles is captured by the fact that the *level spacing* (or *gap*) distributions (the so-called Wigner distributions) have a vanishing density near the origin, whereas for independent points, the gaps follows an exponential distribution (which, in particular, has its mode at the the origin). While persistence diagrams certainly capture point sets in a much more comprehensive manner, the *nnd*-s are much simpler and succinct summaries (albeit more limited), and can be considered as an alternative possibility for comparing point sets when computational load is a bigger consideration than high accuracy.

We examine *nnd*-s in 2D and 3D, which are much less understood than the 1D case. While the *nnd* for a perturbed lattice model can be expressed, in principle, as an infinite series in terms of various Gaussian probabilities, in practice such expressions are of little utility as they do not shed much light on the statistical or analytical properties of the relevant distribution. In this article, we undertake an empirical investigation of the *nnd*-s for perturbed lattice models, comparing them against their counterparts for the Ginibre and the Poisson models, as relevant. Rigorous analytical exploration of their distributional properties, for instance in comparison to the Poisson and the Ginibre models, would be a natural avenue for future research that appears

to be beyond the reach of current methods. We observe in passing that, as σ increases, the nnd-s for perturbed lattice models converge to that of the Poisson, thereby corroborating the overall convergence at the level of point processes.

We do not extensively use nnd-s as a metric for comparison of point sets in our investigations of spatial network models in this paper, we defer the results of the empirical investigations on nnd-s to Appendix B.

5 Disordered lattices for optimal SINR in 2D and 3D

5.1 2D planar networks

The lattice which minimizes the Epstein zeta function in 2D is the triangular lattice, where the fundamental lattice domain is in the shape of a rhombus of unit sidelength in \mathbb{R}^2 ([47, 20, 11, 23, 24]). This is the same as the famous Abrikosov lattice that plays an important role in statistical physics theoretical physics, e.g. through its emergence as the ground state in the celebrated theory of Ginzburg-Landau vortices and Coulomb gases (a.k.a. the 2D one component plasma) ([1, 48, 51, 49]).

For our purposes, we consider Gaussian perturbations of the triangular lattice, with the lattice spacing scaled so as to have on the average one point per unit area. We will refer to this point process as the *Perturbed Triangular Lattice* (abbrv. PTL). We study the coverage probability of these perturbed lattices indexed by the dispersion σ of the Gaussian perturbations, and plot the coverage probability against the corresponding threshold θ .

The coverage probabilities are computed via Monte Carlo simulations, generating a large number of realizations of the random point configurations, computing the corresponding SINR, and obtain the coverage probability from the histogram of SINRs. To be precise, we generate 20,000 samples for each point process (PTL, Ginibre, Poisson) to compute the mean of SINR as a function of θ . Thus, we obtain a family of curves plotting $p_c(\theta)$ against θ , the curves being indexed by the parameter σ . The results are exhibited in Fig. 3 and Fig. 4.

These plots exhibit several interesting features. We empirically observe a strict monotonicity in σ : for $\sigma = 0$, i.e. no disorder, the coverage probability $p_c(\theta)$ is the highest for a given threshold θ , and $p_c(\theta)$ decreases monotonically

as σ increases, always staying above the corresponding curve for the Poisson distribution, but approaching it as $\sigma \rightarrow \infty$.

One of our goals is to obtain a disordered lattice model which can substitute for the random matrix network, both in terms of similarity as point configurations as well as in terms of the behaviour of the SINR. Heuristically, for σ near 0 the model would strongly resemble the original lattice, whereas for σ large, Poissonian behaviour sets in. In particular, when σ is too small, we can trace most points back to the lattice site where it came from, whereas for σ too large, the *memory* of an ordered structure is completely lost. It is natural, therefore, to look for random matrix behaviour somewhere in between, away from these extremities for the disorder parameter. A rule of thumb, therefore, might be to look at disorder of magnitude like half of the lattice spacing, so that the identification of the parent sites for the perturbations of neighbouring lattice points becomes only just improbable.

As discussed in Section 4.1, we compare lattice perturbations with the Ginibre network by comparison of their PDs, which in turn is achieved by computing two alternate metrics. The first metric is their TV distance as atomic probability measures (calculated after smoothing by a localised Gaussian kernel). The second metric is the symmetrized nearest point distance between them. These measures, once again, are computed via Monte Carlo simulations of the point processes, using 100 samples for each value of σ . As unveiled in Fig. 2, it turns out that in both metrics, the closest approximation of the Ginibre network (i.e., the Ginibre network) by a Gaussian Perturbed Triangular Lattice is achieved around $\sigma = 0.4$. In this vein, we make particular note of the relatively sharp convexity of the TV distance curve near its minimum around $\sigma = 0.4$.

The nearest neighbour distributions (abbrv. nnd-s) of the three point processes are displayed in Fig. 10, for the Poisson, Ginibre and PTL for various values of σ . The plots for the nnd-s are generated empirically via Monte Carlo simulations, using 10,000 realizations of the relevant point process for each curve. It may be observed that, as σ increases, the nnd of the corresponding PTL converges to that of the Poisson point process. The closest the nnd for a PTL gets to the nnd of the Ginibre point process is around $\sigma = 0.4$. This is also the perturbation value around which the distance between the corresponding PDs is minimized, and the SINR vs threshold curves nearly overlap.

It may be observed that for $\sigma = 0.4$, the coverage probability curve of the disordered lattice lies close to, and in fact, slightly above the corresponding

curve for the Ginibre network (see Fig. 3 and Fig. 4). This indicates that a wireless network based on a disordered triangular lattice with disorder σ around 0.4 can be taken as an effective replacement for the Ginibre network, in terms of coverage probability for the PTL performing at least as well as the Ginibre. We believe that this can have significant impact on the design and investigation of random wireless networks, particularly from the point of view of large scale numerical and computational research.

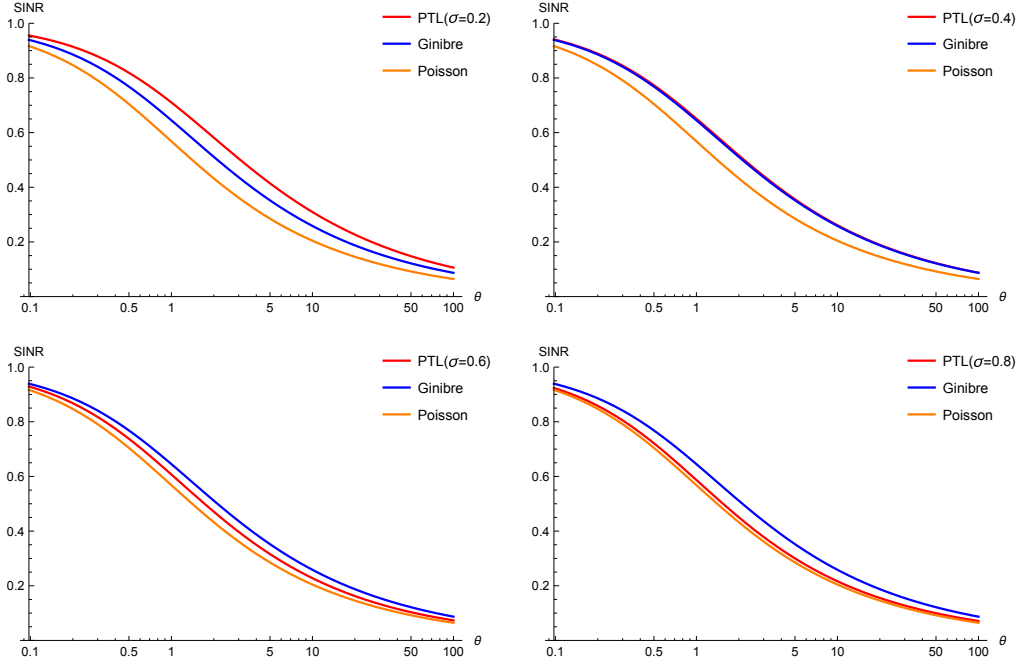


Figure 3: Coverage probability vs SINR threshold curves for Perturbed Triangular Lattice (PTL), Ginibre and Poisson ($\sigma = 0.2, 0.4, 0.6, 0.8$) for $\beta = 2$.

5.2 3D spatial networks

The ordinary cubic lattice has a cube with eight lattice points (i.e., $[0, a]^3$ with a lattice point on each corner) as a unit cell, which is denoted by \mathcal{C} , and it is formed as $\bigcup_{x \in a\mathbb{Z}} (\mathcal{C} + x)$. The unit cell of the Body Centered Cubic (abbrev. BCC) lattice is \mathcal{C} with one more lattice point $(a/2, a/2, a/2)$ in the center and that of Face Centered Cubic (abbrev. FCC) lattice is \mathcal{C} with a lattice point on each face (see (cf. [54, Example 8.3]) for BCC and FCC lattices).

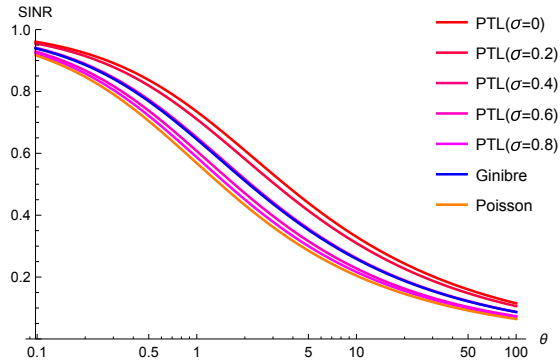


Figure 4: Coverage probability vs SINR threshold curves for Perturbed Triangular Lattice (PTL) ($\sigma = 0, 0.2, 0.4, 0.6, 0.8$), Ginibre, Poisson for $\beta = 2$. Coverage probability curves for PTL decrease as σ increases, match Ginibre, and tend towards that of Poisson.

In 3D Euclidean space, identification of the base lattice to disorder poses a challenge, stemming from the fact that the minimizing lattice for the Epstein zeta function is not fully understood in 3D ([50, 6, 7]). It was shown by Ennola that the FCC lattice as well as the BCC lattice are local minimizers of the Epstein Zeta function in the space of lattices. However, there is no definitive understanding of what the global minimizer is for a given value of s . It was conjectured by Sarnak and Strombergsson that, for $s > 3$ (cf. formula (2.7)), the minimizing lattice for the Epstein Zeta function $\mathcal{E}_\Lambda(s)$ in 3D Euclidean space is the FCC ([50, 6, 7]). In our study, therefore, we will henceforth be using the disordered FCC lattice, leaving the issue of a completely rigorous optimal choice of lattice to future breakthroughs in the theory of lattices.

In our investigations, we consider Gaussian perturbations of the FCC lattice and the cubic lattice (i.e., \mathbb{Z}^3), for various values of the standard deviation σ , and compare them against the Poisson point process of the same intensity in 3D Euclidean space. We plot the coverage probability vs thresholds for networks given by these processes at various values of σ . The plots are generated empirically via Monte Carlo simulations, using 10,000 realizations of the relevant point process for each curve. The results are displayed in Fig. 5 and 6. The plots show the perturbed FCC (abbrv. PFCC) network to be the clearly the best performer for small values of σ , and it is

$p_c(\theta) - \theta$ curve tends to match that of the Perturbed Cubic Lattice (abbrv. PCL) network for larger values of σ starting from around $\sigma = 0.5$, or half the lattice spacing. For all values of σ , however, the PFCC seems to be performing at least as well as the PCL, suggesting that it would be the better choice as the base lattice to perturb.

In Fig. 6, we focus on the behaviour of the $p_c(\theta)$ - θ curve of the PFCC lattice for varying σ , and compare them with the corresponding curve for the Poisson network. We observe worsening performance of the networks with increasing values of σ , reflected in the fact that the curves keep getting pushed down. The Poisson network, for its part, appears to be performing worse compared to the PFCC (as well as the PCL) uniformly for all values of σ , and it is only for large σ that the coverage probability vs threshold curve of the perturbed lattice models tend to converge to that of the Poisson model.

We complement our study by an investigation of the nearest neighbour spacing distributions of these point process in \mathbb{R}^3 . The plots for the nearest neighbour distributions are generated empirically via Monte Carlo simulations, using 10,000 realizations of the relevant point process for each curve. The results are displayed in Fig. 11. It may be observed that the nnd for the PFCC process is in general a bit more concentrated around its mode than the PCL or the Poisson, indicating a more homogeneous distribution of points in space. The Poisson point process, on the other hand, exhibits a very *flat* nnd profile, indicating both clumps of points and large holes. It may also be observed that the nnd curves for the PFCC and the PCL converge around $\sigma = 0.5$, which is also the value of the perturbation at which the coverage probability curves coincide. Finally, for large values of σ the nnd curves for both the perturbed lattice models converge to that of the Poisson, reflecting distributional convergence of the underlying point processes.

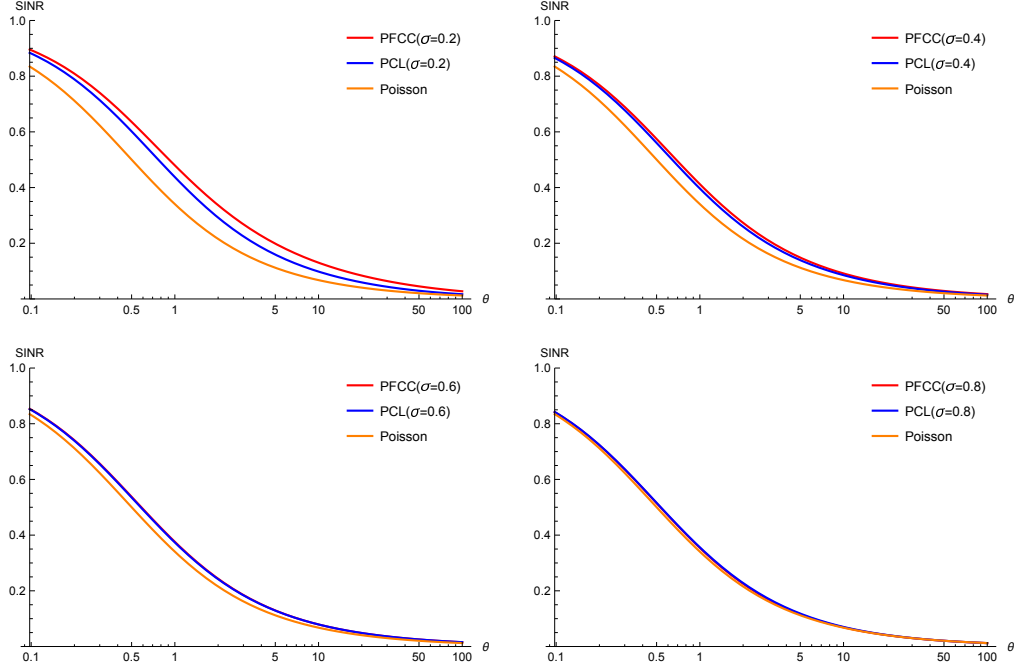


Figure 5: Coverage probability vs SINR threshold curves for Perturbed FCC (PFCC), Perturbed Cubic Lattice (PCL) ($\sigma = 0.2, 0.4, 0.6, 0.8$), Poisson for $\beta = 4/3$.

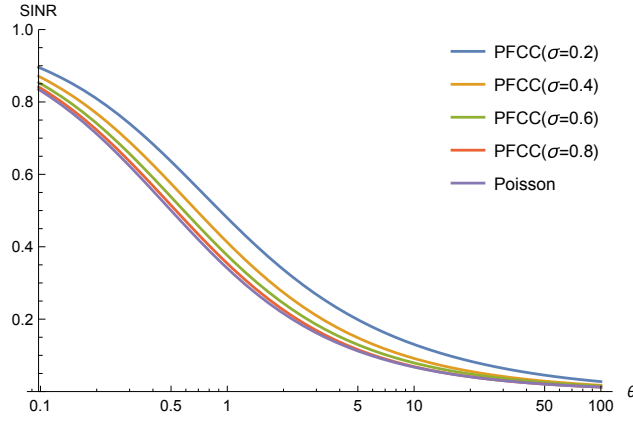


Figure 6: Coverage probability vs SINR threshold curves for Perturbed FCC lattice (PFCC) ($\sigma = 0.2, 0.4, 0.6, 0.8$) from above and Poisson for $\beta = 4/3$. Coverage probability curves for PFCC decrease as σ increases and tend towards that of Poisson.

6 Interpolation with Poisson in the high noise regime

As we have seen in 5.1 and 5.2 for SINR and also Fig. 10 and Fig. 11 in Appendix B for nnd-s of point processes, when the dispersion σ gets large, its SINR and nnd become close to those of Poisson. In this section, we will rigorously demonstrate the convergence of the coverage probabilities of the Gaussian perturbed lattice networks to that of the Poisson network for a given threshold θ , for any starting lattice Λ . In fact, we will establish a more general result in Theorem 6.1. To this end, we introduce the following notation. For any point process \mathcal{P} on \mathbb{R}^d , define the quantity

$$\Sigma_R^\beta(\mathcal{P}) := \sum_{\zeta \in \mathcal{P}: |\zeta| > R} \frac{1}{|\zeta|^{d\beta}}.$$

We are now ready to state

Theorem 6.1. Let $\{\Xi_\sigma\}_{\sigma>0}$ be a collection of point processes on \mathbb{R}^d converging in distribution to a point process Ξ on \mathbb{R}^d as $\sigma \rightarrow \infty$, such that the random variables $\Sigma_R^\beta(\Xi_\sigma) \rightarrow 0$ in probability as $R \rightarrow \infty$, uniformly over the collection $\{\Xi, \{\Xi_\sigma\}_{\sigma>0}\}$. Then, for any $\theta > 0$, the coverage probabilities $p_c(\theta, \Xi_\sigma)$ for Ξ_σ converge, as $\sigma \rightarrow \infty$, to the coverage probability $p_c(\theta, \Xi)$ for the point process Ξ .

We defer the proof of Theorem 6.1 to Section 8. In what follows, we will lay down the argument to demonstrate the convergence to Poisson for perturbed lattice networks in the regime of high noise, using Theorem 6.1.

In order to deduce the convergence of the coverage probabilities of Gaussian lattice perturbations Ξ_σ (with variance σ) to that of the Poisson network σ , we first observe that as $\sigma \rightarrow \infty$, the point processes $\Xi_\sigma \rightarrow \Xi$ in distribution, in the vague topology on the space of locally finite point configurations on \mathbb{R}^d . To see this via a simple dynamical argument, we observe that an infinite system of particles on \mathbb{R}^d , starting at the nodes of a lattice and evolving via non-interacting Brownian motions converges in the long time limit to the homogeneous Poisson point process on \mathbb{R}^d having the same particle density as the initial configuration. For details, we refer the interested reader to [53], in particular to Theorem 2 and Example 2 therein. Now, if we start this dynamics from the initial configuration having one particle each at the lattice sites of Λ , then after time σ , the point configuration evolves to have

the same distribution as the perturbed lattice model at disorder σ . Thus, by virtue of this coupling we observe that, in the limit $\sigma \rightarrow \infty$, the perturbed lattice model converges to the homogeneous Poisson point process.

It, therefore, suffices to establish that the uniform convergence to zero of the tail sums

$$\Sigma_R^\beta(\Xi_\sigma) = \sum_{\zeta \in \Xi_\sigma: |\zeta| > R} \frac{1}{|\zeta|^{d\beta}}.$$

To this end, we may compute the expectation $\mathbb{E}[\Sigma_R^\beta(\mathcal{P})]$ for a translation invariant point process \mathcal{P} on \mathbb{R}^d with unit intensity (i.e., density of points) with respect to Lebesgue measure, and obtain

$$\mathbb{E}[\Sigma_R^\beta(\mathcal{P})] = \int_{\{u \in \mathbb{R}^d: |u| > R\}} \frac{1}{|u|^{d\beta}} du.$$

The last expression clearly converges to 0 as $R \rightarrow \infty$ at a rate that does not depend on the specific point process \mathcal{P} under consideration (thereby leading to uniform convergence in σ in our setting). This establishes the uniform convergence $\mathbb{E}[\Sigma_R^\beta(\Xi_\sigma)] \rightarrow 0$. By Markov's inequality, this implies the desired uniform convergence in probability.

7 Concluding remarks

The problems studied in this work can, as easily, be posed for dimensions $d \geq 3$. In this work, we limit ourselves mostly to dimensions 2 and 3, motivated principally by their relevance to most commonly studied spatial network models. However, perturbed lattices and their network properties do pose an intriguing mathematical challenge in dimensions $d \geq 3$, particularly through the natural connections (in analogy to 2D and 3D) to energy-minimizing lattices. This brings to mind, for example, the case of dimension 24, where the famous Leech Lattice has already been shown to exhibit many remarkable properties - both from the point of view of pure mathematics and also in applications to coding theory and analog-to-digital conversion ([10, 14, 15, 16]). Energy minimizing phenomena for lattices are also known to be relatively well-understood in dimensions 4 and 8 (in addition to dimension 24) ([50, 6, 7]).

8 Proofs of Theorems 1.4 and 6.1

8.1 Proof of Theorem 1.4

We begin by recalling the notation that

$$X_n(\sigma) = n + \sigma\gamma_n, (n \in \Lambda \subset \mathbb{R}^d, \sigma > 0).$$

Let

$$Y_n(\sigma) := |\sigma^{-1}X_n(\sigma)|^2 = \left| \frac{n}{\sigma} + \gamma_n \right|^2.$$

Then $\{Y_n(\sigma)\}$ are independent random variables distributed as follows.

Lemma 8.1. $Y_n(\sigma)$ has the following probability density function

$$f(t, n, \sigma) = e^{-\frac{|n|^2}{2\sigma^2}} \cdot t^{\frac{d}{2}-1} e^{-\frac{1}{2}t} \mathcal{I}_d(\sigma^{-1}|n|\sqrt{t}), \quad (t \geq 0),$$

where $\mathcal{I}_d(u) = \frac{1}{2 \cdot (2\pi)^{d/2}} \int_{\mathbb{S}^{d-1}} e^{u\langle \omega, e_1 \rangle} d\omega$, with e_1 being the first standard co-ordinate vector in \mathbb{R}^d and $d\omega$ being the standard spherical measure on \mathbb{S}^{d-1} .

Proof of Lemma 8.1. For a measurable function F , use a change of variables, we can deduce the following

$$\begin{aligned} \mathbb{E}[F(Y_n(\sigma))] &= \mathbb{E}\left[F\left(\left|\frac{n}{\sigma} + \gamma_n\right|^2\right)\right] \\ &= \int_{\mathbb{R}^d} F(|z|^2) \cdot \frac{1}{(2\pi)^{d/2}} e^{-\frac{1}{2}|z - \frac{n}{\sigma}|^2} dz \\ &= \int_0^\infty \left(\frac{1}{(2\pi)^{d/2}} \int_{\mathbb{S}^{d-1}} F(r^2) e^{-\frac{1}{2}(r^2 + \frac{|n|^2}{\sigma^2} - 2r\frac{|n|}{\sigma}\langle \omega, e_1 \rangle)} d\omega \right) r^{d-1} dr \\ &= \int_0^\infty F(r^2) r^{d-2} e^{-\frac{1}{2}(r^2 + \frac{|n|^2}{\sigma^2})} \mathcal{I}_d(\sigma^{-1}|n|r) \cdot 2r dr \\ &= e^{-\frac{|n|^2}{2\sigma^2}} \int_0^\infty F(t) t^{\frac{d}{2}-1} e^{-\frac{1}{2}t} \mathcal{I}_d(\sigma^{-1}|n|\sqrt{t}) dt \\ &= \int_0^\infty F(t) f(t, n, \sigma) dt, \end{aligned}$$

where, in the third step, we have used the rotation invariance of the standard spherical measure.

This allows us to conclude that $f(t, n, \sigma)$ is the probability density function of $Y_n(\sigma)$. ■

We are now ready to complete the proof of Theorem 1.4.

Proof of Theorem 1.4. (i) In what follows, for simplicity, we will suppress from the notation the dependence on σ . Since $Y_n(\sigma) = |X_n(\sigma)/\sigma|^2$, it is clear that

$$p_c(\theta, \beta, \sigma) = \mathbb{E} \left[\prod_{j \in \Lambda_B} \left(1 + \theta \frac{|X_B|^{d\beta}}{|X_j|^{d\beta}} \right)^{-1} \right] = \mathbb{E} \left[\prod_{j \in \Lambda_B} \left(1 + \theta \frac{Y_B^{d\beta/2}}{Y_j^{d\beta/2}} \right)^{-1} \right].$$

Then it is straightforward to express the coverage probability as follows:

$$\begin{aligned} p_c(\theta, \beta, \sigma) &= \sum_{n \in \Lambda} \mathbb{E} \left[\prod_{j \in \Lambda_n} \left(1 + \theta \frac{Y_n^{d\beta/2}}{Y_j^{d\beta/2}} \right)^{-1}; B = n \right] \\ &= \sum_{n \in \Lambda} \int_0^\infty \mathbb{E} \left[\prod_{j \in \Lambda_n} \left(1 + \theta \frac{t^{d\beta/2}}{Y_j^{d\beta/2}} \right)^{-1}; Y_j \geq t \ (\forall j \neq n) \right] f(t, n, \sigma) dt \\ &= \sum_{n \in \Lambda} \int_0^\infty \prod_{j \in \Lambda_n} \mathbb{E} \left[\left(1 + \theta \frac{t^{d\beta/2}}{Y_j^{d\beta/2}} \right)^{-1}; Y_j \geq t \right] f(t, n, \sigma) dt. \end{aligned} \quad (8.1)$$

We complete the proof of (i) by noting that

$$\mathbb{E} \left[\left(1 + \theta \frac{t^{d\beta/2}}{Y_j^{d\beta/2}} \right)^{-1}; Y_j \geq t \right] = \int_t^\infty \left(1 + \theta \frac{u^{d\beta/2}}{u^{d\beta/2}} \right)^{-1} f(u, j, \sigma) du.$$

(ii) Making a change of variables $t = \theta^{-2/d\beta} s$ in the integral (8.1), we have

$$p_c(\theta, \beta, \sigma) = \sum_{n \in \Lambda} \int_0^\infty \prod_{j \in \Lambda_n} \mathbb{E} \left[\left(1 + \frac{s^{d\beta/2}}{Y_j^{d\beta/2}} \right)^{-1}; Y_j \geq \theta^{-2/d\beta} s \right] f(\theta^{-2/d\beta} s, n, \sigma) \theta^{-2/d\beta} ds.$$

From Lemma 8.1 and (1.9), we deduce that

$$\begin{aligned} \theta^{1/\beta} p_c(\theta, \beta, \sigma) &= \sum_{n \in \Lambda} e^{-\frac{|n|^2}{2\sigma^2}} \int_0^\infty \prod_{j \in \Lambda_n} \mathbb{E} \left[\left(1 + \frac{s^{d\beta/2}}{Y_j^{d\beta/2}} \right)^{-1}; Y_j \geq \theta^{-2/d\beta} s \right] \\ &\quad \times s^{\frac{d}{2}-1} \exp \left(-\frac{1}{2} \theta^{-2/d\beta} s \right) \mathcal{I}_d(\sigma^{-1} |n| \sqrt{\theta^{-2/d\beta} s}) ds \\ &\rightarrow \sum_{n \in \Lambda} e^{-\frac{|n|^2}{2\sigma^2}} \int_0^\infty \prod_{j \in \Lambda_n} \mathbb{E} \left[\left(1 + \frac{s^{d\beta/2}}{Y_j^{d\beta/2}} \right)^{-1} \right] \frac{s^{\frac{d}{2}-1}}{2^{d/2} \Gamma(d/2)} ds \end{aligned} \quad (8.2)$$

as $\theta \rightarrow \infty$. We will justify the interchange of integration and limit in Subsection 8.1.1.

Recalling that the probability density of Y_j is given by $f(\cdot, j, \sigma)$, we obtain the desired result. \blacksquare

8.1.1 Justification of the interchange of integration and limit

We want to justify the interchange of integration and limit in (8.2). Let

$$f_\delta(n, s) := \prod_{j \in \Lambda_n} \mathbb{E} \left[\left(1 + \frac{s^{d\beta/2}}{Y_j^{d\beta/2}} \right)^{-1}; Y_j \geq \delta s \right] s^{\frac{d}{2}-1} \exp \left(-\frac{1}{2} \delta s \right) \mathcal{I}_d(\sigma^{-1}|n|\sqrt{\delta s})$$

and

$$\int f(n, s) \mu(dnds) := \sum_{n \in \Lambda} e^{-\frac{|n|^2}{2\sigma^2}} \int_0^\infty f(n, s) ds.$$

It is easy to see that

$$f_\delta(n, s) \rightarrow \prod_{j \in \Lambda_n} \mathbb{E} \left[\left(1 + \frac{s^{d\beta/2}}{Y_j^{d\beta/2}} \right)^{-1} \right] \frac{s^{\frac{d}{2}-1}}{2^{d/2} \Gamma(d/2)}.$$

By the dominated convergence theorem, it suffices to show that for some $\delta_0 > 0$

$$\int \sup_{0 < \delta < \delta_0} |f_\delta(n, s)| \mu(dnds) < \infty.$$

Lemma 8.2. Let $d \geq 2$. There exist $C_1, C_2 > 0$ such that

$$\prod_{j \in \Lambda_n} \mathbb{E} \left[\left(1 + \frac{s^{d\beta/2}}{Y_j^{d\beta/2}} \right)^{-1} \right] \leq C_1 e^{-C_2 s} \quad \text{for } s \geq 0.$$

Here C_1 and C_2 may depend on σ, d, β but not n .

Proof. We recall that $Y_j = |j/\sigma + \eta|^2$ where η is a d -dimensional standard Gaussian random variables. Then, $\mathbb{E}Y_j = |j/\sigma|^2 + d$. For $0 < c_1 < c_2$, let

$$\Lambda_{n, c_1, c_2} := \{j \in \Lambda_n : c_1 s \leq \mathbb{E}Y_j \leq c_2 s\}$$

and for $a > 0$, which is chosen later, let

$$B_a = \bigcap_{j \in \Lambda_{n, c_1, c_2}} \{Y_j \leq a \mathbb{E}Y_j\}.$$

On B_a , since $Y_j \leq a\mathbb{E}Y_j \leq ac_2s$ for $j \in \Lambda_{n,c_1,c_2}$, we have

$$\begin{aligned} \mathbb{E} \left[\prod_{j \in \Lambda_{n,c_1,c_2}} \left(1 + \frac{s^{d\beta/2}}{Y_j^{d\beta/2}} \right)^{-1}; B_a \right] &\leq \mathbb{E} \left[\prod_{j \in \Lambda_{n,c_1,c_2}} \left(1 + (ac_2)^{-d\beta/2} \right)^{-1}; B_a \right] \\ &\leq e^{-\alpha c_3 s^{d/2}}. \end{aligned} \quad (8.3)$$

where $\alpha = \log(1 + (ac_2)^{-d\beta/2}) > 0$ and we used the fact that $|\Lambda_{n,c_1,c_2}| \geq c_3 s^{d/2}$ for any sufficiently large s . On B_a^c , for any sufficiently large s ,

$$\mathbb{E} \left[\prod_{j \in \Lambda_{n,c_1,c_2}} \left(1 + \frac{s^{d\beta/2}}{Y_j^{d\beta/2}} \right)^{-1}; B_a^c \right] \leq \mathbb{P}(B_a^c) \leq \sum_{j \in \Lambda_{n,c_1,c_2}} P(Y_j > ac_1s).$$

Since $|j/\sigma|^2 \leq c_2s$ for $j \in \Lambda_{n,c_1,c_2}$, we see that

$$ac_1s < Y_j = |j/\sigma + \eta|^2 \leq 2(|j/\sigma|^2 + |\eta|^2) \leq 2(c_2s + |\eta|^2)$$

and, by taking $a = 2(c_2 + 1)/c_1$, we have

$$\begin{aligned} P(Y_j > ac_1s) &\leq P \left(\frac{1}{2}(ac_1 - 2c_2)s \leq |\eta|^2 \right) \\ &= P(|\eta|^2 > s) \\ &\sim \frac{1}{\Gamma(d/2)} \left(\frac{s}{2} \right)^{d/2-1} e^{-s/2} \quad \text{as } s \rightarrow \infty, \end{aligned}$$

where $|\eta|^2$ is the χ_d^2 -distribution with d degrees of freedom (see (2.10)). Thus,

$$\mathbb{E} \left[\prod_{j \in \Lambda_{n,c_1,c_2}} \left(1 + \frac{s^{d\beta/2}}{Y_j^{d\beta/2}} \right)^{-1}; B_a^c \right] \leq c_5 s^{d-1} e^{-s/2}. \quad (8.4)$$

Therefore, (8.3) with $d \geq 2$ and (8.4) yield

$$\begin{aligned} \prod_{j \in \Lambda_n} \mathbb{E} \left[\left(1 + \frac{s^{d\beta/2}}{Y_j^{d\beta/2}} \right)^{-1} \right] &\leq \mathbb{E} \left[\prod_{j \in \Lambda_{n,c_1,c_2}} \left(1 + \frac{s^{d\beta/2}}{Y_j^{d\beta/2}} \right)^{-1} \right] \\ &\leq C_1 \exp(-C_2s). \end{aligned}$$

This completes the proof. ■

Since $\mathcal{I}_d(u) \leq \mathcal{I}_d(0)e^u$ for every $u \geq 0$, we have

$$\begin{aligned} |f_\delta(n, s)| &= \prod_{j \in \Lambda_n} \mathbb{E} \left[\left(1 + \frac{s^{d\beta/2}}{Y_j^{d\beta/2}} \right)^{-1} \right] s^{\frac{d}{2}-1} e^{-\delta s/2} \mathcal{I}_d(\sigma^{-1}|n|\sqrt{\delta s}) \\ &\leq C_1 e^{-C_2 s} \cdot s^{\frac{d}{2}-1} \mathcal{I}_d(0) e^{b\sqrt{\delta s}} \leq C e^{-cs} e^{b\sqrt{\delta s}}, \end{aligned} \quad (8.5)$$

where $b = |n|/\sigma$. From (8.5), by taking δ_0 small enough, we have

$$\begin{aligned} \int_0^\infty \sup_{0 < \delta < \delta_0} |f_\delta(n, s)| ds &\leq C \int_0^\infty e^{-cs} e^{b\sqrt{\delta_0 s}} ds \\ &= C \left\{ \frac{1}{c} + \frac{b\sqrt{\delta_0} e^{\frac{\delta_0}{4c} b^2} \sqrt{\pi}}{2c^{3/2}} \left(1 + \operatorname{Erf} \left(\frac{b\sqrt{\delta_0}}{2\sqrt{c}} \right) \right) \right\} \\ &\leq C' e^{\frac{b^2}{4}} = C' e^{\frac{|n|^2}{4\sigma^2}}, \end{aligned}$$

where $\operatorname{Erf}(z) = \frac{2}{\sqrt{\pi}} \int_0^z e^{-t^2} dt$. Hence

$$\int \sup_{0 < \delta < \delta_0} |f_\delta(n, s)| \mu(dnds) \leq C' \sum_{n \in \Lambda} e^{-\frac{|n|^2}{4\sigma^2}} < \infty,$$

which justifies that the order of limit and integration can be interchanged.

8.2 Proof of Theorem 6.1

Proof of Theorem 6.1. We use the following expression, which holds for any point process Λ :

$$p_c(\theta, \Lambda) = \mathbb{E}_\Lambda \left[\prod_{\lambda \in \Lambda_{\mathbf{B}}} \left(1 + \theta \cdot \frac{|X_{\mathbf{B}}|^{d\beta}}{|X_\lambda|^{d\beta}} \right)^{-1} \right]$$

Let $B(0; R)$ denote the ball of radius R in \mathbb{R}^d . Fix such an $R > 0$, to be thought of as large. Consider a compactly supported smooth radial function $\varphi : \mathbb{R}^d \rightarrow [0, 1]$, such that $\varphi(x) = 1$ if $x \in B(0; R)$, and $\varphi(x)$ decreases to 0 as $|x| \rightarrow \infty$. Consider the following functional $p_c(\theta, \Lambda, R)$ that is associated with $p_c(\theta, \Lambda)$

$$p_c(\theta, \Lambda, R) = \mathbb{E}_\Lambda \left[\prod_{\lambda \in \Lambda_{\mathbf{B}}} \left(1 + \theta \cdot \frac{|X_{\mathbf{B}} \varphi(X_\lambda)|^{d\beta}}{|X_\lambda|^{d\beta}} \right)^{-1} \right].$$

Observe that the functional $\prod_{\lambda \in \Lambda_{\mathbf{B}}} \left(1 + \theta \cdot \frac{|X_{\mathbf{B}}\varphi(X_{\lambda})|^{d\beta}}{|X_{\lambda}|^{d\beta}}\right)^{-1}$ is continuous on the space of point configurations on \mathbb{R}^d , where the latter is endowed with the *vague topology* on the space of locally finite point configurations on \mathbb{R}^d , entailing convergence as discrete measures on compact sets. Furthermore, this functional is bounded by 1. These two facts, together with convergence in distribution of Ξ_{σ} to Ξ implies that, for any fixed $R > 0$, we have $p_c(\theta, \Xi_{\sigma}, R) \rightarrow p_c(\theta, \Xi, R)$ as $\sigma \rightarrow \infty$. Now, let $\Lambda \in \{\Xi, \{\Xi_{\sigma}\}_{\sigma > 0}\}$. Let Λ_B^R denote $\Lambda \cap B(0; R)$ and $\Lambda_B^{R^c}$ denote $\Lambda \cap B(0; R)^c$.

Let $g_{\theta}(x) = (1 + \theta|x|^{d\beta})^{-1}$. Then we have,

$$\begin{aligned}
& |p_c(\theta, \Lambda) - p_c(\theta, \Lambda, R)| \\
&= \left| \mathbb{E}_{\Lambda} \left[\prod_{\lambda \in \Lambda_B^R} g_{\theta}\left(\frac{|X_{\mathbf{B}}|}{|X_{\lambda}|}\right) \left(\prod_{\lambda \in \Lambda_B^{R^c}} g_{\theta}\left(\frac{|X_{\mathbf{B}}|}{|X_{\lambda}|}\right) - \prod_{\lambda \in \Lambda_B^{R^c}} g_{\theta}\left(\frac{|X_{\mathbf{B}}\varphi(X_{\lambda})|}{|X_{\lambda}|}\right) \right) \right] \right| \\
&\leq \mathbb{E}_{\Lambda} \left[\left| \prod_{\lambda \in \Lambda_B^{R^c}} g_{\theta}\left(\frac{|X_{\mathbf{B}}|}{|X_{\lambda}|}\right) - \prod_{\lambda \in \Lambda_B^{R^c}} g_{\theta}\left(\frac{|X_{\mathbf{B}}\varphi(X_{\lambda})|}{|X_{\lambda}|}\right) \right| \right] \\
&\leq \mathbb{E}_{\Lambda} \left[\left| \prod_{\lambda \in \Lambda_B^{R^c}} g_{\theta}\left(\frac{|X_{\mathbf{B}}|}{|X_{\lambda}|}\right) - 1 \right| \right] + \mathbb{E}_{\Lambda} \left[\left| \prod_{\lambda \in \Lambda_B^{R^c}} g_{\theta}\left(\frac{|X_{\mathbf{B}}\varphi(X_{\lambda})|}{|X_{\lambda}|}\right) - 1 \right| \right]
\end{aligned} \tag{8.6}$$

Now we observe that

$$\prod_{\lambda \in \Lambda_B^{R^c}} g_{\theta}\left(\frac{|X_{\mathbf{B}}|}{|X_{\lambda}|}\right)^{-1} \leq \prod_{\lambda \in \Lambda_B^{R^c}} \exp\left(\theta \frac{|X_{\mathbf{B}}|^{d\beta}}{|X_{\lambda}|^{d\beta}}\right) = \exp\left(\theta |X_{\mathbf{B}}|^{d\beta} \Sigma_R^{\beta}(\Lambda)\right).$$

Since $|\varphi(X_{\lambda})| \leq 1$, we may also deduce that

$$\prod_{\lambda \in \Lambda_B^{R^c}} g_{\theta}\left(\frac{|X_{\mathbf{B}}\varphi(X_{\lambda})|}{|X_{\lambda}|}\right)^{-1} \leq \exp\left(\theta |X_{\mathbf{B}}|^{d\beta} \Sigma_R^{\beta}(\Lambda)\right).$$

This implies that

$$\min \left\{ \prod_{\lambda \in \Lambda_{\mathbf{B}}^{R^c}} g_{\theta} \left(\frac{|X_{\mathbf{B}}|}{|X_{\lambda}|} \right), \prod_{\lambda \in \Lambda_{\mathbf{B}}^{R^c}} g_{\theta} \left(\frac{|X_{\mathbf{B}} \varphi(X_{\lambda})|}{|X_{\lambda}|} \right) \right\} \geq \exp \left(-\theta |X_{\mathbf{B}}|^{d\beta} \Sigma_R^{\beta}(\Lambda) \right). \quad (8.7)$$

On the other hand,

$$\max \left\{ \prod_{\lambda \in \Lambda_{\mathbf{B}}^{R^c}} g_{\theta} \left(\frac{|X_{\mathbf{B}}|}{|X_{\lambda}|} \right), \prod_{\lambda \in \Lambda_{\mathbf{B}}^{R^c}} g_{\theta} \left(\frac{|X_{\mathbf{B}} \varphi(X_{\lambda})|}{|X_{\lambda}|} \right) \right\} \leq 1. \quad (8.8)$$

As a consequence of (8.7) and (8.8), we deduce that

$$\begin{aligned} & \mathbb{E}_{\Lambda} \left[\left| \prod_{\lambda \in \Lambda_{\mathbf{B}}^{R^c}} g_{\theta} \left(\frac{|X_{\mathbf{B}}|}{|X_{\lambda}|} \right) - 1 \right| \right] + \mathbb{E}_{\Lambda} \left[\left| \prod_{\lambda \in \Lambda_{\mathbf{B}}^{R^c}} g_{\theta} \left(\frac{|X_{\mathbf{B}} \varphi(X_{\lambda})|}{|X_{\lambda}|} \right) - 1 \right| \right] \\ & \leq 2 \mathbb{E}_{\Lambda} \left[1 - \exp \left(-\theta |X_{\mathbf{B}}|^{d\beta} \Sigma_R^{\beta}(\Lambda) \right) \right], \end{aligned}$$

which converges to 0 as $R \rightarrow \infty$ uniformly over $\Lambda \in \{\Xi, \{\Xi_{\sigma}\}_{\sigma>0}\}$ because of the uniform convergence $\Sigma_R^{\beta}(\Lambda) \rightarrow 0$ (as $R \rightarrow \infty$).

In light of (8.6), this implies that we can choose R and σ (depending on R) large enough such that

$$\begin{aligned} & |p_c(\theta, \Xi_{\sigma}) - p_c(\theta, \Xi)| \\ & \leq |p_c(\theta, \Xi_{\sigma}) - p_c(\theta, \Xi_{\sigma}, R)| + |p_c(\theta, \Xi_{\sigma}, R) - p_c(\theta, \Xi, R)| + |p_c(\theta, \Xi, R) - p_c(\theta, \Xi)| \end{aligned}$$

can be made arbitrarily small. Thus, as $\sigma \rightarrow \infty$, we have the convergence of coverage probabilities $p_c(\theta, \Xi_{\sigma}) \rightarrow p_c(\theta, \Xi)$. This completes the proof of our result. \blacksquare

9 Acknowledgements

We would like to thank Joel L. Lebowitz and Khanh Duy Trinh for illuminating discussions regarding this work, and the anonymous referees for their insightful comments and suggestions. SG was supported in part by the MOE grants R-146-000-250-133, R-146-000-312-114 and MOE-T2EP20121-0013. NM was supported in part by the Grant-in-Aid for Scientific Research

(C) (No.19K11838) of the Japan Society for the Promotion of Science (JSPS). TS was supported in part by the Grant-in-Aid for Scientific Research (B) (No.18H01124) and (S) (No.16H06338) of Japan Society for the Promotion of Science (JSPS) and by JST CREST Mathematics (15656429).

Appendix

A Appendix : Persistent homology and persistence diagrams

In this appendix, we briefly recall the definition of persistent homology and persistence diagram. We refer the readers to (cf. [66, 21, 61, 33]) and references therein for more details.

Let V be a finite set and we simply write $V = \{1, 2, \dots, n\}$. An abstract simplicial complex over V is a collection K of subsets which is closed under the operation of taking non-empty subsets, i.e., if $\sigma \in K$ and $(\emptyset \neq) \eta \subset \sigma$, then $\eta \in K$. An element $\sigma \in K$ is called a q -simplex if the cardinality of $|\sigma| = q + 1$. A 0-simplex is a vertex, 1-simplex is an edge, 2-simplex is a face, and so on. We denote the set of q -simplices by K_q . We introduce an equivalence relation on ordered simplices by $(i_0, \dots, i_q) \sim (j_0, \dots, j_q)$ if there exists an even permutation $\pi \in \mathcal{S}_{q+1}$ such that $j_k = \pi(i_k)$ for every $k = 0, 1, \dots, q$. There are two equivalence classes, which are called orientations. When $\sigma = \{i_0, \dots, i_q\}$, we denote by $\langle \sigma \rangle$ the equivalence class to which the ordered simplex (i_0, \dots, i_q) belongs. When (i_0, \dots, i_q) and (j_0, \dots, j_q) have different orientations, we put minus sign as $\langle i_0, \dots, i_q \rangle = -\langle j_0, \dots, j_q \rangle$. For example, $\langle 1, 3, 2 \rangle = -\langle 1, 2, 3 \rangle$, $\langle 1, 4, 3, 2 \rangle = -\langle 1, 2, 3, 4 \rangle$. Let \mathbb{F} be a field and we define the q -chain group by

$$C_q(K) := \left\{ \sum_{\sigma \in K_q} a_\sigma \langle \sigma \rangle : a_\sigma \in \mathbb{F} \right\},$$

which is an \mathbb{F} -vector space having a basis $\{\langle \sigma \rangle : \sigma \in K_q\}$. Let $\partial_q : C_q(K) \rightarrow C_{q-1}(K)$ be a linear map (boundary map) defined by

$$\partial_q \langle i_0, i_1, \dots, i_q \rangle = \sum_{k=0}^q (-1)^k \langle i_0, \dots, \widehat{i_k}, \dots, i_q \rangle$$

where \widehat{i}_k means the removal of i_k , and it is extended linearly for general elements of $C_q(K)$ by $\partial_q(\sum_{\sigma \in K_q} a_\sigma \langle \sigma \rangle) = \sum_{\sigma \in K_q} a_\sigma \partial_q(\langle \sigma \rangle)$. It is easy to see that $\partial_q \circ \partial_{q+1} = 0$ for every q . The chain groups and boundary maps are assembled into a chain complex:

$$\cdots \rightarrow C_q(K) \xrightarrow{\partial_q} C_{q-1}(K) \xrightarrow{\partial_{q-1}} \cdots \xrightarrow{\partial_2} C_1(K) \xrightarrow{\partial_1} C_0(K) \xrightarrow{\partial_0} 0$$

From the relation $\partial_q \circ \partial_{q+1} = 0$, we have $\text{Im } \partial_{q+1} \subset \ker \partial_q$. Then one can define the q th-homology group by

$$H_q(K) := \ker \partial_q / \text{Im } \partial_{q+1},$$

which is the quotient \mathbb{F} -vector space. Each generator of $H_q(K)$ represents a q -dimensional hole.

A filtration $\mathbb{K} = \{K_t\}_{t=0}^n$ of simplicial complexes is an increasing family of simplicial complexes $K_0 \subset K_1 \subset \cdots \subset K_n$. For each simplicial complex K_t , the homology group $H_q(K_t)$ is defined as above. So a family of homology groups $\{H_q(K_t)\}_{t=0}^n$ has an information about how q -dimensional holes change as t varies. But, one can observe more information, persistence, by employing persistent homology. Since we have a filtration, we have an inclusion $\iota_t : K_t \rightarrow K_{t+1}$, which induces the linear maps $(\iota_t)_*$ on homology groups $\{H_q(K_t)\}_{t=0}^n$:

$$H_q(K_0) \xrightarrow{(\iota_0)^*} \cdots \xrightarrow{(\iota_{t-1})^*} H_q(K_t) \xrightarrow{(\iota_t)^*} H_q(K_{t+1}) \xrightarrow{(\iota_{t+1})^*} \cdots \xrightarrow{(\iota_{T-1})^*} H_q(K_n), \quad (\text{A.1})$$

which is called a *persistence module*, denoted by $H_q(\mathbb{K})$. A collection of vector spaces $\{V_t\}_{t=0}^n$ and linear maps $f_{st} : V_s \rightarrow V_t$ such that $f_{st} \circ f_{tu} = f_{su}$ for $s < t < u$ is called a representation of A_n -quiver. In the persistence module above, $f_{st} = (\iota_t) \circ \cdots \circ (\iota_s)_*$ and $V_t = H_q(K_t)$. A basic representation of A_n -quiver is an *interval module* $I(b, d)$ defined by

$$0 \xrightarrow{g_0} \cdots \rightarrow 0 \xrightarrow{g_{b-1}} \mathbb{F} \xrightarrow{g_b} \mathbb{F} \xrightarrow{g_{b+1}} \cdots \rightarrow \mathbb{F} \xrightarrow{g_{d-1}} 0 \rightarrow \cdots \xrightarrow{g_n} 0,$$

where $g_t = \text{id}_{\mathbb{F}}$ is the identity map on \mathbb{F} for $t = b, b+1, \dots, d-2$. From the theory of representations of A_n -quiver, we have the following decomposition property.

Theorem A.1. ([66]) Let $H_q(\mathbb{K})$ be a persistence module of the form (A.1). There uniquely exist indices $p \in \mathbb{Z}_{\geq 0}$ and $b_i, d_i \in \{0, 1, \dots, n\}$ with $0 \leq b_i < d_i \leq n, i = 1, 2, \dots, p$ such that the following isomorphism holds:

$$H_q(\mathbb{K}) \simeq \bigoplus_{i=1}^p I(b_i, d_i) \quad (\text{A.2})$$

We can interpret the interval module $I(b_i, d_i)$ as persistence of the i th generator of q th homology group, which appears at time b_i and disappears at time d_i . In order to visualize the information (A.2) of the decomposition of $H_q(\mathbb{K})$, we denote its persistence diagram by

$$D_q(\mathbb{K}) := \{(b_i, d_i) : i = 1, 2, \dots, p\} \subset \Delta,$$

which is a multiset in $\Delta := \{(x, y) \in \mathbb{R}^2 : 0 \leq x < y \leq \infty\}$. See Fig. 8.

Example A.2. We consider an example of a filtration given in Fig. 7. We can observe that there is a cycle (1-dimensional hole) at time 1, two independent cycles at time 2, and a cycle at time 3. It is also considered that a cycle appears at time 1, another cycle appears at time $t = 2$, one cycle disappears at time 3 and 4. This reflects on the persistent module (over a field \mathbb{R}) as

$$\begin{aligned} H_1(\mathbb{K}) &:= H_1(K_0) \rightarrow H_1(K_1) \rightarrow H_1(K_2) \rightarrow H_1(K_3) \rightarrow H_1(K_4) \\ &\simeq 0 \rightarrow \mathbb{R} \rightarrow \mathbb{R}^2 \rightarrow \mathbb{R} \rightarrow 0. \end{aligned}$$

In this case, we can see that

$$H_1(\mathbb{K}) \simeq I(1, 4) \oplus I(2, 3) \simeq (0 \rightarrow \mathbb{R} \rightarrow \mathbb{R} \rightarrow \mathbb{R} \rightarrow 0) \oplus (0 \rightarrow 0 \rightarrow \mathbb{R} \rightarrow 0 \rightarrow 0),$$

although we have another possibility of decomposition by interval modules as

$$H_1(\mathbb{K}) \simeq I(1, 3) \oplus I(2, 4) \simeq (0 \rightarrow \mathbb{R} \rightarrow \mathbb{R} \rightarrow 0 \rightarrow 0) \oplus (0 \rightarrow 0 \rightarrow \mathbb{R} \rightarrow \mathbb{R} \rightarrow 0).$$

One cannot observe this distinction of decompositions if one only has the homology groups $\{H_q(K_t)\}_{t=0}^n$. This is a consequence of induced linear maps $\{(i_t)_*\}_{t=0}^n$ which comes from the inclusions of the filtration \mathbb{K} . So the persistent homology has more information than the collection of homology groups do. We remark that here in this example, we treat index t as time, but it is sometimes treated as resolution or other parameters, depending on what we are looking at. In the Čech filtration defined below, the radius r is such a parameter.

Given $\Phi = \{x_1, x_2, \dots, x_N\} \subset \mathbb{R}^d$ and $r > 0$, we define a Čech complex built over Φ by

$$K(\Phi, r) := \{\sigma \subset \Phi : \bigcap_{x \in \sigma} B(x, r) \neq \emptyset\},$$

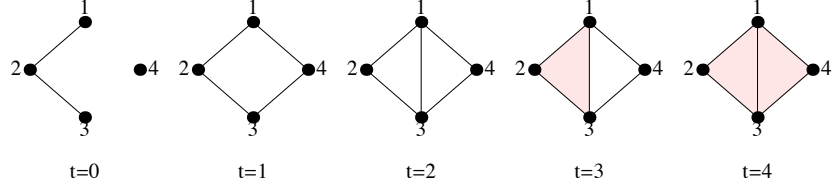


Figure 7: Filtration. $\{1, 2, 3\}$ and $\{1, 3, 4\}$ are 2-simplices and colored in pink at time 3 and 4.

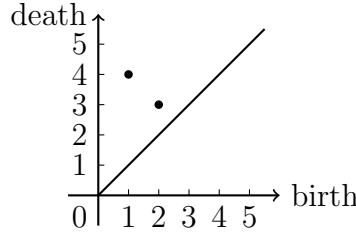


Figure 8: Persistence diagram of $H_1(\mathbb{K})$ for the filtration given in Fig. 7.

where $B(x, r)$ is the ball of radius r centered at x . A collection $\mathbb{K}(\Phi) := \{K(\Phi, r)\}_{r \geq 0}$ is an increasing family of Čech complexes, which we call Čech filtration over Φ . From the Čech filtration, we have the persistent homology $H_q(\mathbb{K}(\Phi))$ by Theorem A.1 and its persistence diagram. Here we deal with a filtration with continuous parameter r , but for a finite configuration Φ , the birth of simplices occurs only at discrete finite parameters $r_1 < r_2 < \dots < r_n$ so that we can apply Theorem A.1 to this case and define its persistence diagrams supported on $\{r_1, \dots, r_n\} \cap \Delta$ in an obvious way.

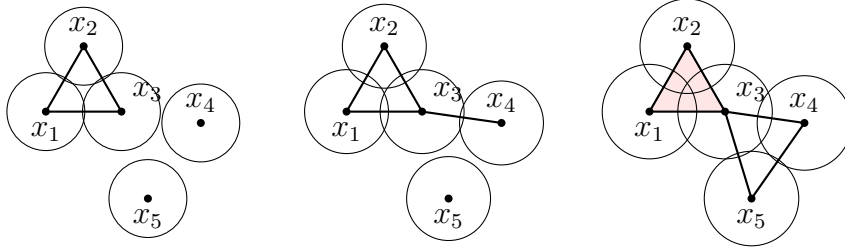


Figure 9: Čech complexes $K(\Phi, r)$ over $\Phi = \{x_1, x_2, \dots, x_5\}$ as r increases.

B Appendix : Comparison of nnd-s of 2D & 3D point sets

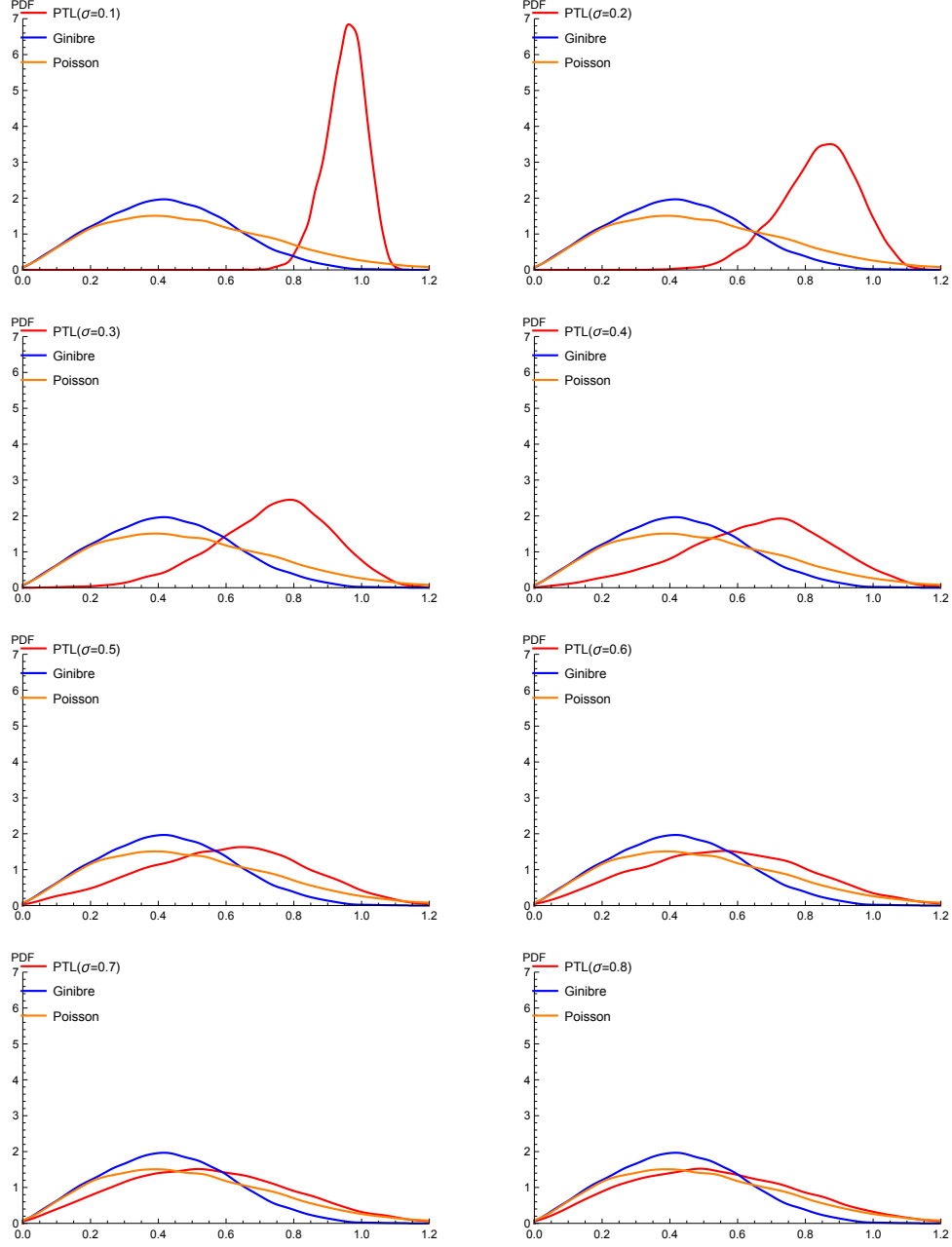


Figure 10: Nearest neighbour distribution for Perturbed Triangular Lattice (PTL), Ginibre and Poisson ($\sigma = 0.1, 0.2, \dots, 0.8$) for $\beta = 2$.

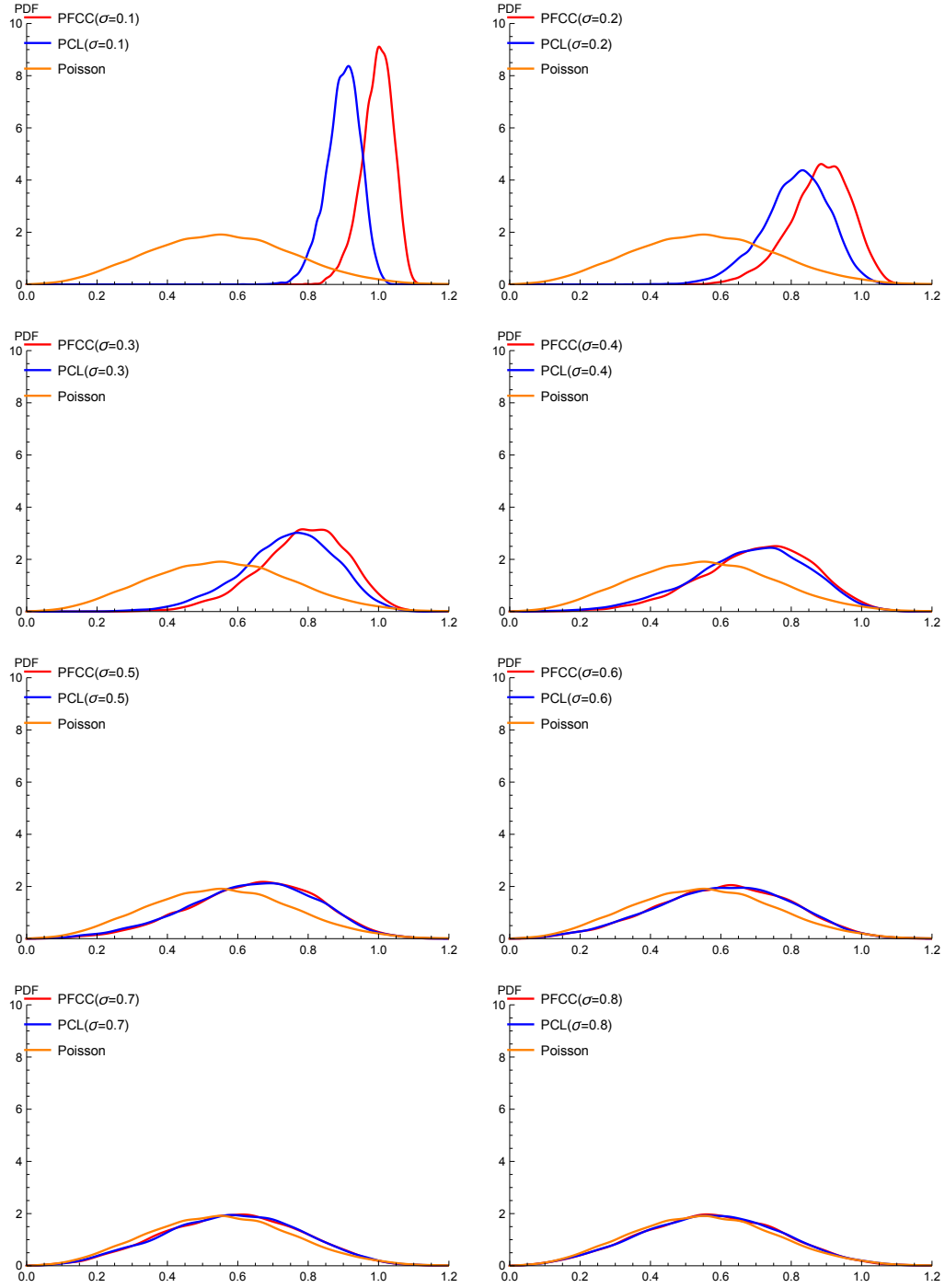


Figure 11: Nearest neighbour distribution for perturbed Face-centered cubic lattice (PFCC), Perturbed Cubic Lattice(PCL) and Poisson ($\sigma = 0.1, 0.2, \dots, 0.8$) for $\beta = 2$.

References

- [1] Alexei Alexeyevich Abrikosov. The magnetic properties of superconducting alloys. *Journal of Physics and Chemistry of Solids*, 2(3):199–208, 1957.
- [2] Jeffrey G Andrews, Radha Krishna Ganti, Martin Haenggi, Nihar Jindal, and Steven Weber. A primer on spatial modeling and analysis in wireless networks. *IEEE Communications Magazine*, 48(11):156–163, 2010.
- [3] Michael Baake, Holger Koesters, and Robert V Moody. Diffraction theory of point processes: Systems with clumping and repulsion. *Journal of Statistical Physics*, 159(4):915–936, 2015.
- [4] Francois Baccelli and Bartłomiej Błaszczyszyn. *Stochastic geometry and wireless networks*, volume 1. Now Publishers Inc, 2010.
- [5] Marc Barthélemy. Spatial networks. *Physics Reports*, 499(1-3):1–101, 2011.
- [6] Laurent Betermin. Minimization of lattice energies : From old to new results in dimensions 2 and 3. OPCOP 2017, CIEM, Castro Urdiales, 2017.
- [7] Laurent Bétermin. Local optimality of cubic lattices for interaction energies. *Analysis and Mathematical Physics*, 9(1):403–426, 2019.
- [8] Xavier Blanc and Mathieu Lewin. The crystallization conjecture: a review. *arXiv preprint arXiv:1504.01153*, 2015.
- [9] Bartłomiej Błaszczyszyn, Martin Haenggi, Paul Keeler, and Sayandev Mukherjee. *Stochastic geometry analysis of cellular networks*. Cambridge University Press, 2018.
- [10] Richard Ewen Borcherds. The leech lattice. *Proceedings of the Royal Society of London. A. Mathematical and Physical Sciences*, 398(1815):365–376, 1985.
- [11] John WS Cassels. On a problem of rankin about the epstein zeta-function. *Glasgow Mathematical Journal*, 4(2):73–80, 1959.

- [12] Sarvadaman Chowla and Atle Selberg. On epstein’s zeta function (i). *Proceedings of the National Academy of Sciences of the United States of America*, 35(7):371, 1949.
- [13] David Cohen-Steiner, Herbert Edelsbrunner, and John Harer. Stability of persistence diagrams. *Discrete & computational geometry*, 37(1):103–120, 2007.
- [14] Henry Cohn, Abhinav Kumar, Stephen D Miller, Danylo Radchenko, and Maryna Viazovska. The sphere packing problem in dimension 24. *Annals of Mathematics*, pages 1017–1033, 2017.
- [15] John Conway and NJAA Sloane. Soft decoding techniques for codes and lattices, including the golay code and the leech lattice. *IEEE Transactions on Information Theory*, 32(1):41–50, 1986.
- [16] John Horton Conway and Neil James Alexander Sloane. *Sphere packings, lattices and groups*, volume 290. Springer Science & Business Media, 2013.
- [17] Na Deng, Wuyang Zhou, and Martin Haenggi. The ginibre point process as a model for wireless networks with repulsion. *IEEE Transactions on Wireless Communications*, 14(1):107–121, 2014.
- [18] Carl P Dettmann. New horizons in multidimensional diffusion: the lorentz gas and the riemann hypothesis. *Journal of Statistical Physics*, 146(1):181–204, 2012.
- [19] Carl P Dettmann, Orestis Georgiou, and Pete Pratt. Spatial networks with wireless applications. *Comptes Rendus Physique*, 19(4):187–204, 2018.
- [20] PH Diananda. Notes on two lemmas concerning the epstein zeta-function. *Glasgow Mathematical Journal*, 6(4):202–204, 1964.
- [21] Herbert Edelsbrunner and John Harer. Persistent homology-a survey. *Contemporary mathematics*, 453:257–282, 2008.
- [22] Emilio Elizalde. *Ten physical applications of spectral zeta functions*, volume 855. Springer, 2012.

- [23] Veikko Ennola. A lemma about the epstein zeta-function. *Glasgow Mathematical Journal*, 6(4):198–201, 1964.
- [24] Veikko Ennola. On a problem about the epstein zeta-function. In *Mathematical Proceedings of The Cambridge Philosophical Society*, volume 60, pages 855–875. Cambridge University Press, 1964.
- [25] Laszlo Erdos and Horng-Tzer Yau. Universality of local spectral statistics of random matrices. *Bulletin of the American Mathematical Society*, 49(3):377–414, 2012.
- [26] Subhro Ghosh and Joel Lebowitz. Number rigidity in superhomogeneous random point fields. *Journal of Statistical Physics*, 166(3-4):1016–1027, 2017.
- [27] Subhroshekhar Ghosh and Joel L Lebowitz. Fluctuations, large deviations and rigidity in hyperuniform systems: a brief survey. *Indian Journal of Pure and Applied Mathematics*, 48(4):609–631, 2017.
- [28] Subhroshekhar Ghosh and Joel L Lebowitz. Generalized stealthy hyperuniform processes: Maximal rigidity and the bounded holes conjecture. *Communications in Mathematical Physics*, 363(1):97–110, 2018.
- [29] Jean Ginibre. Statistical ensembles of complex, quaternion, and real matrices. *Journal of Mathematical Physics*, 6(3):440–449, 1965.
- [30] Peter J Grabner. Point sets of minimal energy. In Gerhard Larcher, Friedrich Pillichshammer, Arne Winterhof, and Chaoping Xing, editors, *Applied algebra and number theory*. Cambridge University Press, 2014.
- [31] M. Haenggi. The meta distribution of the sir in poisson bipolar and cellular networks. *IEEE Transactions on Wireless Communications*, 15(4):2577–2589, 2016.
- [32] Martin Haenggi. *Stochastic geometry for wireless networks*. Cambridge University Press, 2012.
- [33] Yasuaki Hiraoka, Tomoyuki Shirai, and Khanh Duy Trinh. Limit theorems for persistence diagrams. *Ann. Appl. Probab.*, 28(5):2740–2780, 10 2018.

- [34] John Ben Hough, Manjunath Krishnapur, Yuval Peres, et al. *Zeros of Gaussian analytic functions and determinantal point processes*, volume 51. American Mathematical Soc., 2009.
- [35] B Jancovici, Joel L Lebowitz, and G Manificat. Large charge fluctuations in classical coulomb systems. *Journal of statistical physics*, 72(3-4):773–787, 1993.
- [36] Norman L Johnson, Samuel Kotz, and Narayanaswamy Balakrishnan. *Continuous univariate distributions*. John Wiley & Sons, Ltd, 1995.
- [37] Olav Kallenberg. *Foundations of modern probability*. Springer Science & Business Media, 2006.
- [38] Robert Kleinberg. Geographic routing using hyperbolic space. In *IEEE INFOCOM 2007-26th IEEE International Conference on Computer Communications*, pages 1902–1909. IEEE, 2007.
- [39] Genki Kusano, Yasuaki Hiraoka, and Kenji Fukumizu. Persistence weighted gaussian kernel for topological data analysis. volume 48 of *Proceedings of Machine Learning Research*, pages 2004–2013, New York, New York, USA, 20–22 Jun 2016. PMLR.
- [40] Nikolaj N. Lebedev. *Special functions and their applications*. Dover, 1972.
- [41] Yingzhe Li, Francois Baccelli, Harpreet S. Dhillon, and Jeffrey G. Andrews. Fitting determinantal point processes to macro base station deployments. In *IEEE Global Communications Conference, GLOBECOM 2014, Austin, TX, USA, December 8-12, 2014*, pages 3641–3646. IEEE, 2014.
- [42] Jorge Mateu, Frederic P Schoenberg, and D Diez. On distances between point patterns and their applications. *American Statistician*, in review, 9, 2010.
- [43] Madan Lal Mehta. *Random matrices*. Elsevier, 2004.
- [44] Naoto Miyoshi and Tomoyuki Shirai. A cellular network model with gini-bre configured base stations. *Advances in Applied Probability*, 46(3):832–845, 2014.

- [45] Naoto Miyoshi and Tomoyuki Shirai. Cellular networks with alpha-ginibre configured base stations. In *The Impact of Applications on Mathematics*, pages 211–226. Springer, 2014.
- [46] S Sundhar Ram, D Manjunath, Srikanth K Iyer, and D Yogeshwaran. On the path coverage properties of random sensor networks. *IEEE Transactions on Mobile Computing*, 6(5):494–506, 2007.
- [47] Robert Alexander Rankin. A minimum problem for the epstein zeta-function. *Glasgow Mathematical Journal*, 1(4):149–158, 1953.
- [48] Etienne Sandier and Sylvia Serfaty. *Vortices in the magnetic Ginzburg-Landau model*, volume 70. Springer Science & Business Media, 2008.
- [49] Etienne Sandier, Sylvia Serfaty, et al. 2d coulomb gases and the renormalized energy. *The Annals of Probability*, 43(4):2026–2083, 2015.
- [50] Peter Sarnak and Andreas Strömbergsson. Minima of epstein’s zeta function and heights of flat tori. *Inventiones mathematicae*, 165(1):115–151, 2006.
- [51] Sylvia Serfaty. *Coulomb gases and Ginzburg–Landau vortices*. 2015.
- [52] Tomoyuki Shirai and Yoichiro Takahashi. Random point fields associated with certain fredholm determinants i: fermion, poisson and boson point processes. *Journal of Functional Analysis*, 205(2):414 – 463, 2003.
- [53] Charles Stone. On a theorem by dobrushin. *The Annals of Mathematical Statistics*, 39(5):1391–1401, 1968.
- [54] Toshikazu Sunada. *Topological crystallography*, volume 6 of *Surveys and Tutorials in the Applied Mathematical Sciences*. Springer, Tokyo, 2013. With a view towards discrete geometric analysis.
- [55] Terence Tao, Van Vu, et al. Random matrices: universality of local eigenvalue statistics. *Acta mathematica*, 206(1):127–204, 2011.
- [56] Audrey Terras. *Harmonic analysis on symmetric spaces and applications I & II*. Springer Science & Business Media, 2012.

- [57] Edward Charles Titchmarsh, Edward Charles Titchmarsh Titchmarsh, DR Heath-Brown, et al. *The theory of the Riemann zeta-function*. Oxford University Press, 1986.
- [58] Salvatore Torquato. Hyperuniform states of matter. *Physics Reports*, 745:1–95, 2018.
- [59] Salvatore Torquato and Frank H Stillinger. Local density fluctuations, hyperuniformity, and order metrics. *Physical Review E*, 68(4):041113, 2003.
- [60] Salvatore Torquato, Ge Zhang, and Frank H Stillinger. Ensemble theory for stealthy hyperuniform disordered ground states. *Physical Review X*, 5(2):021020, 2015.
- [61] Shmuel Weinberger. What is... persistent homology. *Notices of the AMS*, 58(1):36–39, 2011.
- [62] Eugene P Wigner. Characteristic vectors of bordered matrices with infinite dimensions. *Annals of Mathematics*, pages 548–564, 1955.
- [63] Eugene P Wigner. Random matrices in physics. *SIAM review*, 9(1):1–23, 1967.
- [64] Feng Yan, Philippe Martins, and Laurent Decreusefond. Accuracy of homology based coverage hole detection for wireless sensor networks on sphere. *IEEE transactions on wireless communications*, 13(7):3583–3595, 2014.
- [65] D Yogeshwaran, Robert J Adler, et al. On the topology of random complexes built over stationary point processes. *The Annals of Applied Probability*, 25(6):3338–3380, 2015.
- [66] Afra Zomorodian and Gunnar Carlsson. Computing persistent homology. *Discrete & Computational Geometry*, 33(2):249–274, 2005.